CAR T expansion and systemic inflammation: diverging impacts on large B-cell lymphoma therapy in the multicenter CART SIE study

Martina Magni,[1*] Sadhana Jonnalagadda,[1*] Francesca Bonifazi,[2] Massimiliano Bonafé,[2,3] Silva Ljevar,[4] Giada Zanirato,[1] Serena De Matteis,[2] Federico Stella,[5] Angelica Barone,[1,5] Giulia Bertolini,[6] Anisa Bermema,[1] Annalisa Chiappella,[1] Maria Chiara Tisi,[7] Ilaria Cutini,[8] Mattia Novo,[9] Giovanni Grillo,[10] Mirko Farina,[11] Massimo Martino,[12] Mauro Krampera,[13] Massimo Massaia,[14] Luca Arcaini,[15,16] Stefania Bramanti,[17] Pier Luigi Zinzani,[2,3] Anna Dodero,[1] Paolo Corradini[1,5#] and Cristiana Carniti[1#]

[1]Hematology Division, Fondazione IRCCS Istituto Nazionale dei Tumori di Milano, Milan; [2]IRCCS Azienda Ospedaliero-Universitaria di Bologna, Istituto di Ematologia "Seràgnoli", Bologna; [3]Department of Medical and Surgical Sciences (DIMEC), University of Bologna, Bologna; [4]Unit of Biostatistics for Clinical Research, Department of Data Science, Fondazione IRCCS Istituto Nazionale dei Tumori di Milano, Milan; [5]School of Medicine, Università degli Studi di Milano, Milan; [6]Unit of Epigenomics and Biomarkers of Solid Tumors, Department of Experimental Oncology, Fondazione IRCCS Istituto Nazionale dei Tumori di Milano, Milan; [7]Hematology Unit, San Bortolo Hospital, Vicenza; [8]SOD Terapie Cellulari e Medicina Trasfusionale, AAD Trapianto di Midollo Osseo, Ospedale Careggi, Florence; [9]SC Ematologia, AOU Città della Salute e della Scienza, Torino; [10]Dipartimento di Ematologia e Trapianto di Midollo, ASST Grande Ospedale Metropolitano Niguarda, Milan; [11]Unit of Blood Disease and Bone Marrow Transplantation, and Unit of Hematology, University of Brescia, ASST Spedali Civili di Brescia, Brescia; [12]Hematology and Stem Cell Transplantation and Cellular Therapies Unit (CTMO), Department of Hemato-Oncology and Radiotherapy, Grande Ospedale Metropolitano "Bianchi-Melacrino-Morelli", Reggio Calabria; [13]Hematology and Bone Marrow Transplant Unit, Section of Biomedicine of Innovation, Department of Engineering for Innovative Medicine (DIMI), University of Verona, Verona; [14]Division of Hematology - AO S. Croce e Carle, Cuneo and Laboratory of Blood Tumor Immunology, Molecular Biotechnology Center "Guido Tarone", University of Torino, Torino; [15]Department of Molecular Medicine, University of Pavia, Pavia; [16]Division of Hematology, Fondazione IRCCS Policlinico San Matteo, Pavia and [17]Department of Oncology/Hematology, IRCCS Humanitas Research Hospital, Milan, Italy

**MMag and SJ contributed equally as first authors.*
#CC and PC contributed equally as senior authors.

Correspondence: C. Carniti
cristiana.carniti@istitutotumori.mi.it

Received: February 12, 2025.
Accepted: May 19, 2025.
Early view: May 29, 2025.

https://doi.org/10.3324/haematol.2025.287528

Chimeric Antigen Receptor T-cell expansion and systemic inflammation: diverging impacts on large B-cell lymphoma therapy in the multicenter CART SIE study

Supplementary data

Supplementary methods

Multiparameter flow cytometry (MFC)

CAR T enumeration

Circulating CAR T cells were monitored extensively using multiparameter flow cytometry (MFC) on days 5, 7, 10, 14, 21, and 30 post-infusion, with monthly follow-ups until CAR T cells were no longer detectable. For this analysis, 262 Large B-cell Lymphoma (LBCL) patients were selected from the CART SIE cohort based on the availability of biological samples and paired clinical data (at least three post-infusion time-points for circulating CAR T level assessment). The identification of circulating CAR T cells was performed with the CD19 CAR Detection Reagent (Miltenyi Biotec) as previously described [1]. Briefly, 100 µl of peripheral blood (PB) was stained following the manufacturer's instruction and red blood cells (RBC) were lysed using Ammonium Chloride Lysing solution (BD Biosciences, Franklin Lakes, NJ, USA). Then, the resulting white blood cells were labeled with the following antibodies (all from Miltenyi Biotec): biotin-PE (clone REA746), CD45-VioBlue (clone REA747), CD3-FITC (clone REA613), CD4-VioGreen (clone REA623), CD8-APC-Vio770 (clone REA734), CD14-APC (clone REA599) and 7-AAD staining solution. CAR T-cell detection in infusion products followed previously described methods [1].

A known limitation of the CD19 CAR Detection Reagent is a background signal generated by the biotin-PE antibody used for labeling. This signal was subtracted as previously described to avoid overestimating CAR T-cell counts [1]. Alternatively, CAR T-cell enumeration was performed using the CD19 CAR idiotype antibody (CD19 CAR FMC63, Miltenyi Biotec). In this method, 100 µl of PB was lysed and labeled with a cocktail of antibodies, including CD19 CAR FMC63-PE, CD45-VioBlue, CD3-FITC, CD4-VioGreen, CD8-APC-Vio7, CD14-APC and 7-AAD staining solution. CAR T-cell counts obtained using these two reagents (CD19 CAR Detection Reagent with biotin subtraction and CD19 CAR FMC63) were highly correlated (Supplementary Figure 2), supporting the use of both methods within the same study.

Differentiation and Exhaustion Status

For CAR T-cell differentiation status analysis, cells were labelled with the following antibodies (all from Miltenyi Biotec): CD3-FITC, CD19 CAR-PE, CD4-VioGreen, CD8-APC-Vio770, CD45RO-APC (clone REA611), CD62L-PE-Vio700 (clone 145/15), CD197-VioBlue (clone REA546). To evaluate CAR T-cell exhaustion, cells were labeled with CD3 FITC, CAR-PE, CD4-VioGreen, CD8-APC-Vio770, CD223 (LAG-3)-VioBlue (clone REA351), CD366 (TIM-3)-APC (clone REA635) and CD279 (PD-1)-PeVio770 (clone REA1165). CAR T-cell differentiation status analysis in leukapheresis products was performed as previously described [2].

Data Acquisition and Analysis

CAR T-cell enumeration was performed using a MACSQuant Analyzer MQ10 or MQ16 (Miltenyi Biotec), and analyzed with the MACSQuantify software. Custom analysis protocols (Express Mode Master Package for absolute quantification of cells, Miltenyi Biotec) or predefined optimized settings for CAR T-cell analysis were applied. The gating strategy used included exclusion of debris and selection of CD45+, viable, CD3+ and CAR+ cells as previously described [1]. Among identified CAR T cells, CD4 and CD8 expression was further evaluated. For the characterization of CAR T-cell differentiation and exhaustion states, data were acquired on BD FACSCanto II (BD Biosciences) and analyzed using FlowJo-v10 software.

gDNA and cfDNA extraction

Genomic DNA (gDNA) was isolated from infusion product leftovers, PB, bone marrow (BM) and tissue samples using the NucleoSpin Tissue kit (Macherey-Nagel) and quantified with the benchtop fluorimeter Qubit 2.0 (Thermo Fisher Scientific), using the high sensitive Qubit dsDNA HS Assay Kit (Thermo Fisher Scientific). Cell free DNA (cfDNA) was extracted from 2 ml of plasma for each time point using the Qiagen Circulating Nucleic Acid Kit (Qiagen) and quality was assessed using the Agilent Cell-free DNA ScreeTape kit on the 4200 TapeStation System (Agilent Technologies).

Droplet digital PCR (ddPCR)

Development of a ddPCR assay for CAR T-cell detection and enumeration

Partial cDNA sequences of tisa-cel and axi-cel CAR constructs were obtained using gDNA extracted from infusion product leftovers. A common region between products was identified to generate a unique assay. Sequences of primers are reported in Supplementary table 3. Experiments involving CAR-positive samples (infusion product leftovers and PB from infused patients) and CAR-negative controls (PB from healthy donors and lymphoma patients prior to CAR T infusion) showed a very good separation between positive and negative droplets, allowing us to set positive thresholds (Supplementary Figure 5A). According to these thresholds, the assay showed an excellent specificity (Supplementary Figure 5B). These threshold values were applied to further experiments, to increase standardization.

The assay displayed a high inter-assay reproducibility when tested on different samples for each product, with a broad range of CAR copies concentrations (3.05E+01 – 5.12E+05 CAR copies/µg DNA) (Supplementary Figure 6). Sensitivity was assessed by performing a dilution of approximately 10000 tisa-cel and axi-cel CAR copy vectors spiked in 66 ng of healthy donor gDNA (or 10000 diploid genome equivalents) which were then subjected to 1:10 serial dilutions. Target sequences were detectable up to the 0.01% dilution with a highly significant linear correlation between measured and expected values (linear regression R2 = 1.000, $p < 0.0001$ for tisa-cel and R2 = 0.9999, $p < 0.0001$ for axi-cel) (Supplementary Figure 7), demonstrating a limit of detection of 1 CAR copy in a background of 10000 cells.
This primer-probe assay can be used to quantify tisa-cel and axi-cel CAR copies also in qPCR experiments, with highly comparable results (supplementary Figure 8).

The Bio-Rad QX200™ ddPCR System was used for all ddPCR experiments analyzing gDNA and cfDNA for CAR copy number evaluation. CD19-CAR-vectors were detected using primers and FAM-labeled-probes, which were designed and developed by us. Albumin was detected using a custom HEX-labeled assay (cod. 10031279, Bio-Rad) and used as reference gene (REF) to estimate the amount of genomic material in each reaction. The reaction mix for the number of reactions needed was prepared according to the manufacturers' instructions. A CAR-negative gDNA sample and a Non-Template Control (NTC) were included in each run. Droplets were formed using the Droplet Generator (Bio-Rad), thermocycled at 95°C for 10 min, followed by 40 cycles at 95°C for 30 s and 60°C for 1 min, 10 min at 98°C in the end and an infinite hold at 10°C on the SimpliAmp Thermal Cycler (Thermo Fisher Scientific). Droplets were read and analyzed by the QX200TM Droplet Reader and QuantaSoftTM software (Bio-Rad) following manufacturer's recommendations. Data from less than 12000 droplets were discarded for concentration calculation. The 2-D plot view was used to set the threshold for both FAM and HEX channels.
After assuming that 1 REF copy corresponded to a half genome (ca. 3.3E-06µg), CD19-CAR vector copy numbers were expressed as CAR copies/µg DNA. The following calculations were applied:

$$\text{tot REF copies/reaction} = \text{REF copies/µL} \times 20\ \text{µL}$$
$$\text{tot CAR copies/reaction} = \text{CARcopies/µL} \times 20\ \text{µL}$$
$$\text{tot gDNA/reaction} = \text{tot REF copies/reaction} \times 3.3\text{E-}06\text{µg}$$
$$\text{CAR copies/µg} = (\text{tot CAR copies/reaction})/(\text{tot gDNA/reaction})$$

Evaluation of transduction efficiency of T lymphocytes
To evaluate the transduction efficiency of T lymphocytes, we integrated MFC and ddPCR data to estimate the CAR vector copy number (VCN) per CAR T cell in infusion products. First, the percentage of CAR+ among CD45+ hematopoietic cells, identified by MFC, was used to calculate the number of CAR T cells within each ddPCR reaction and then these values allowed us to evaluate the CAR VCN/CAR T cell.

RT-qPCR

Our in house primer-probe assay can be used to quantify tisa-cel and axi-cel CAR copies also in RT-qPCR (Supplementary Figure 8). RT-qPCR was performed in a total volume of 20 µl. PCR mix was prepared with 10 µl of TaqMan Universal Master Mix II, with Uracil N-glycosylase (UNG) enzyme (Applied Biosystem), 0.6 µl of 10 µM forward and reverse primers (final concentration 300nM), 0.6 µl of 5 µM FAM-labeled CAR19-probe (final concentration 150nM), 22 ng of gDNA and nuclease-free water to adjust the mix to the final volume. The amplification was carried out at 50°C for 2 mins, 95°C for 10 mins, 40 cycles of 95°C for 15s and 60 °C for 1 min. All samples were run in triplicate into 96-well plates on the QuantStudio™ 7 Flex Real Time PCR System (Thermo Fisher Scientific). Quantification was performed using the standard curve method.

ELISA

To isolate plasma for cytokines analyses, peripheral blood samples were collected in EDTA tubes and centrifuged at 1000g for 15 min, within 30 minutes of collection. Plasma samples were immediately stored at -80 °C. IL-1β, IL-6, IL-10, IL-11, IL-18, TGF-β, IFN-γ and TNF-α present in the plasma samples were quantified using the automatic ELISA instrument ELLA (Protein Simple), according to the manufacturer's instructions. The detection limit of the assays were: 0.064 pg/mL for IL-1β, 0.11 pg/mL for IL-6, 0.14 pg/mL for IL-10, 0.2 pg/mL for IL-18, 2.0 pg/mL for IL-11, 5.29 pg/mL for TGF-β, 0.05 pg/mL for IFN-γ, 0.03 pg/mL for TNF-α.

Statistical Analyses

Graphs and statistical analyses were performed with GraphPad Prism version 9.3.1. Time of CAR T-cell administration was used as origin in all time-to-event analyses. For group comparison of categorical data Chi-Squared test was used. Two-tailed Spearman correlation test was applied to compare continuous variables. Mann-Whitney or Kruskal-Wallis tests were used to compare variables for independent groups. Linear regression analysis was used for molecular assay sensitivity tests. All reported P values (P) are two-sided and are statistically significant when $P<0.05$.

Overall survival (OS) was defined as the time from CAR T infusion to death from any cause, with censoring at the last follow-up for patients who were still alive.

Progression-free survival (PFS) was defined as the time from CAR T infusion to either disease progression or death, whichever occurred first, with censoring at the last follow-up for patients alive without progression.

The associations between OS, PFS, and potential risk factors were assessed using univariable and multivariable Cox proportional hazards models. The response to treatment and the incidence of adverse events were analyzed using logistic regression models. Kaplan-Meier estimate with the log-rank test was used for survival curves.

Lactate dehydrogenase (LDH), ferritin, and C-reactive protein (CRP) were all treated as continuous variables in both univariate and multivariable models. The odds ratios (in the logistic models) and hazard ratios (in the Cox proportional hazards models) were used to compare risk associated with each biomarker at its 75th percentile (third quartile) versus its 25th percentile (first quartile).

Cut-off values for CAR T count at day 10 post-infusion (C_{10}), at peak expansion (C_{max}), and the median cumulative CAR T level within the first month ($AUC_{0\text{-}30}$) were determined using receiver operating characteristic (ROC) curves. The optimal cut-off was defined as the value corresponding to the point closest to (0, 1) on the ROC curve. For survival outcomes, the ROC curve at 12 months was used.

Supplementary Figure 1

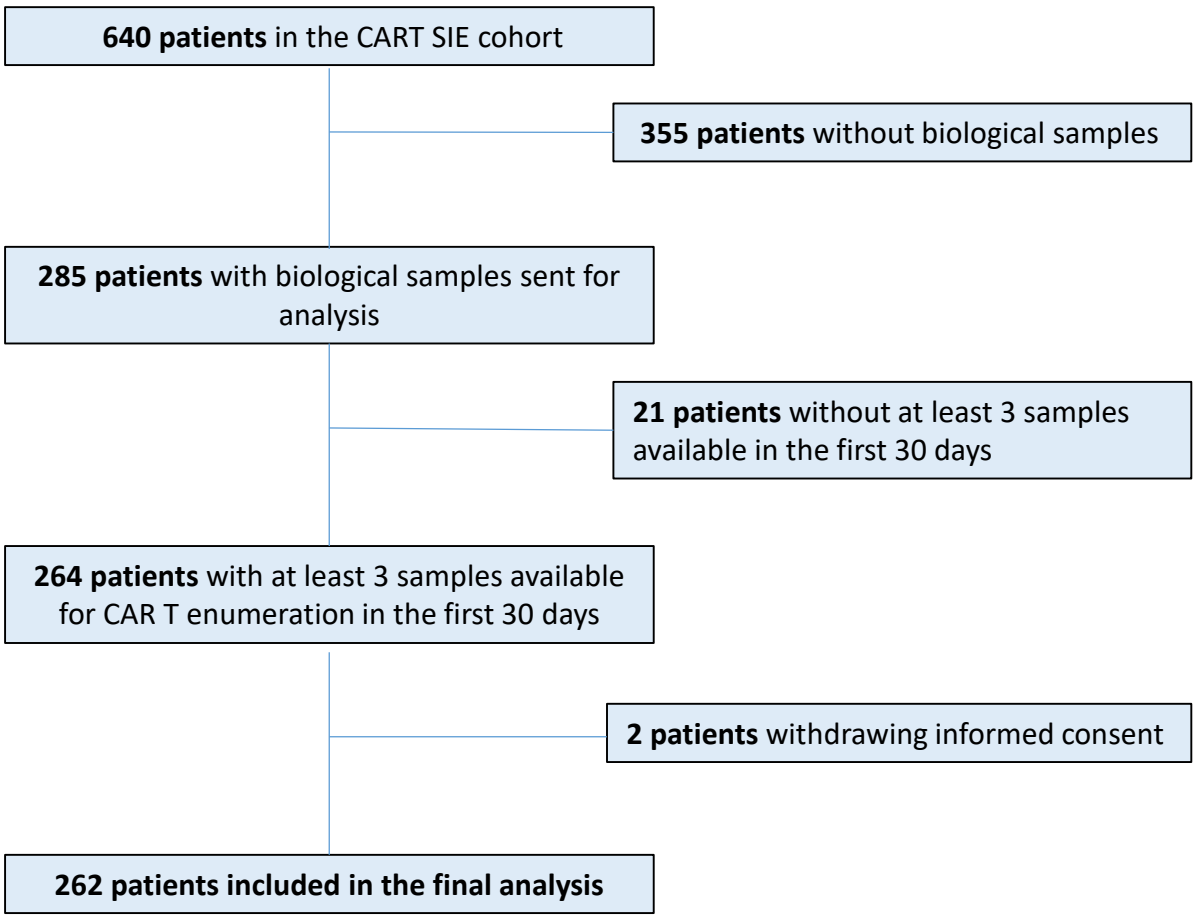

Supplementary Figure 1: Flow chart detailing the number of patients included in the study and the reasons for exclusions.

Supplementary Figure 2

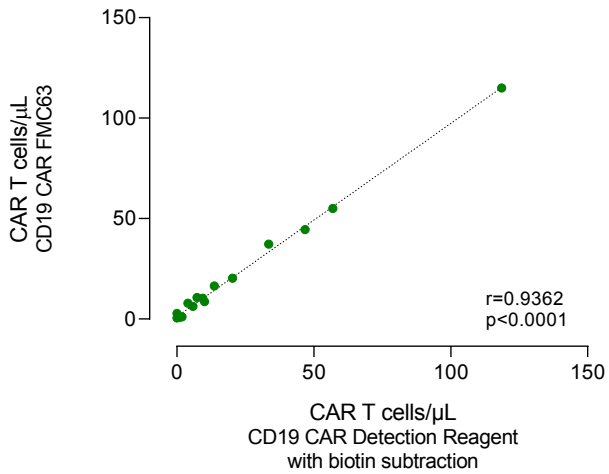

Supplementary Figure 2: Comparison of multiparameter flow cytometry (MFC) reagents for CAR T-cell enumeration.

Scatter dot plot showing the Spearman correlation between CAR T-cell enumeration performed with the idiotype antibody CD19 CAR FMC63 and the CD19 CAR detection reagent, with biotin background subtraction (n=20).

Supplementary Figure 3

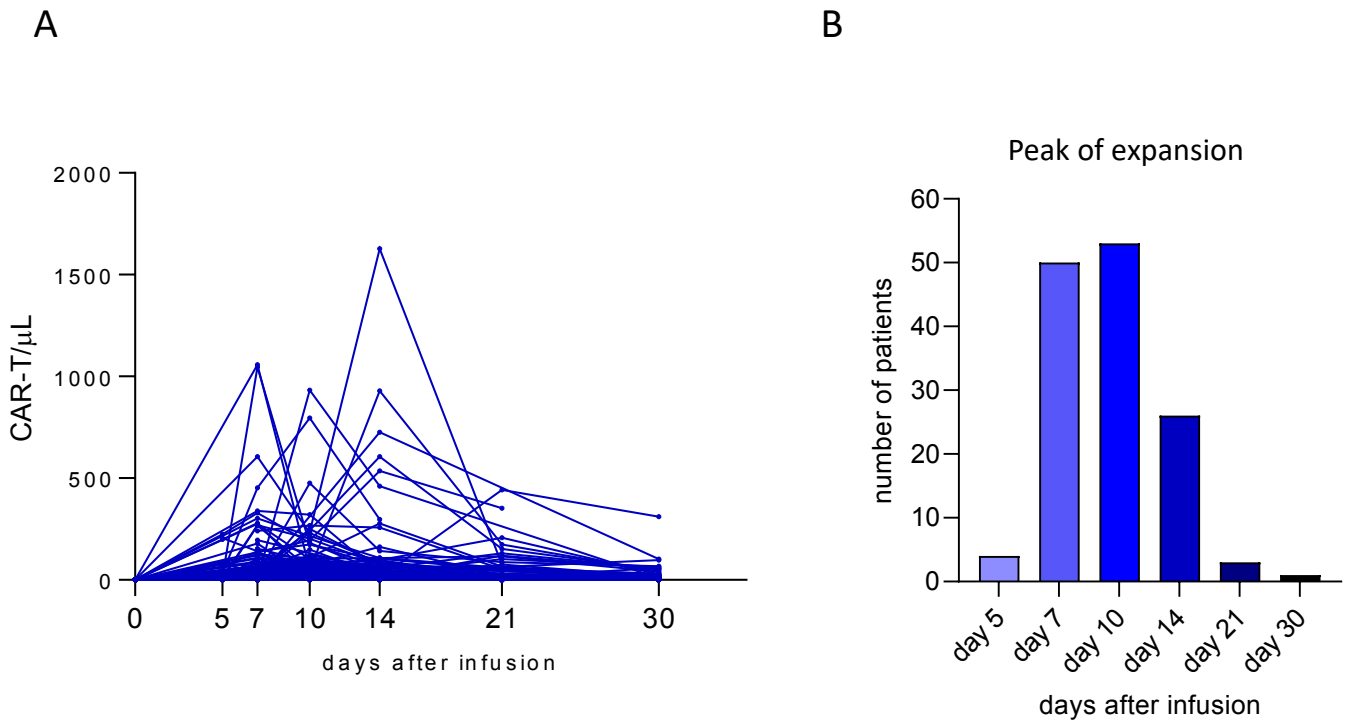

Supplementary Figure 3: in vivo CAR T-cell expansion kinetics by multiparameter flow cytometry (MFC).
A) in vivo expansion kinetics within the first month after infusion. **B)** analysis of the peak of CAR T expansion, in those patients with complete expansion kinetics (n=137).

Supplementary Figure 4

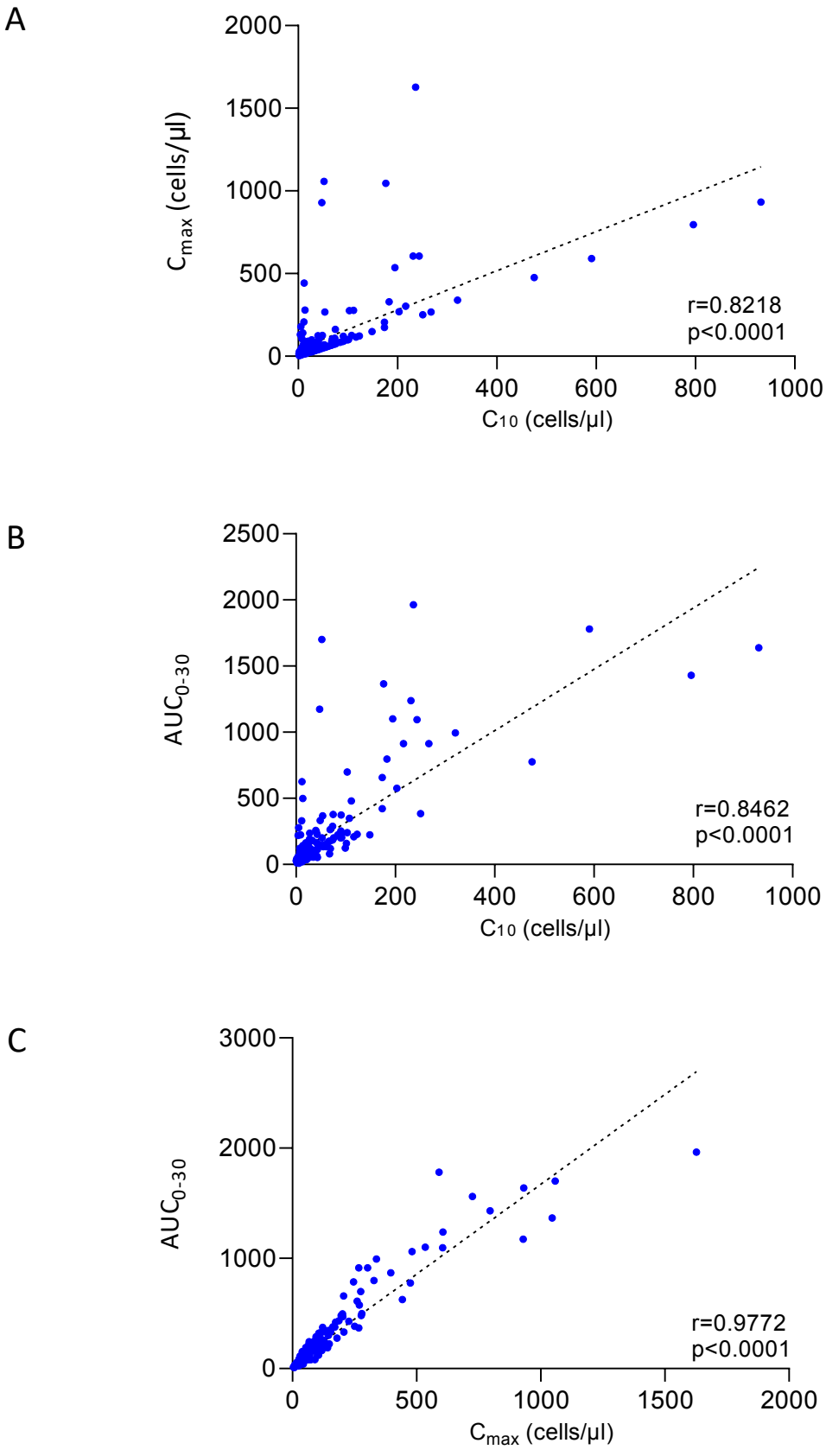

Supplementary Figure 4: Kinetic parameters evaluated by multiparameter flow cytometry (MFC) were strongly correlated.

Scatter dot plots showing the Spearman correlations between: **A)** CAR T count at day 10 post-infusion (C_{10}) and at peak expansion (C_{max}) (n=167); **B)** CAR T count at day 10 post-infusion (C_{10}) and median cumulative CAR T level within the first month (AUC_{0-30}) (n=167); **C)** CAR T count at peak expansion (C_{max}) and median cumulative CAR T level within the first month (AUC_{0-30}) (n=262).

Supplementary Figure 5

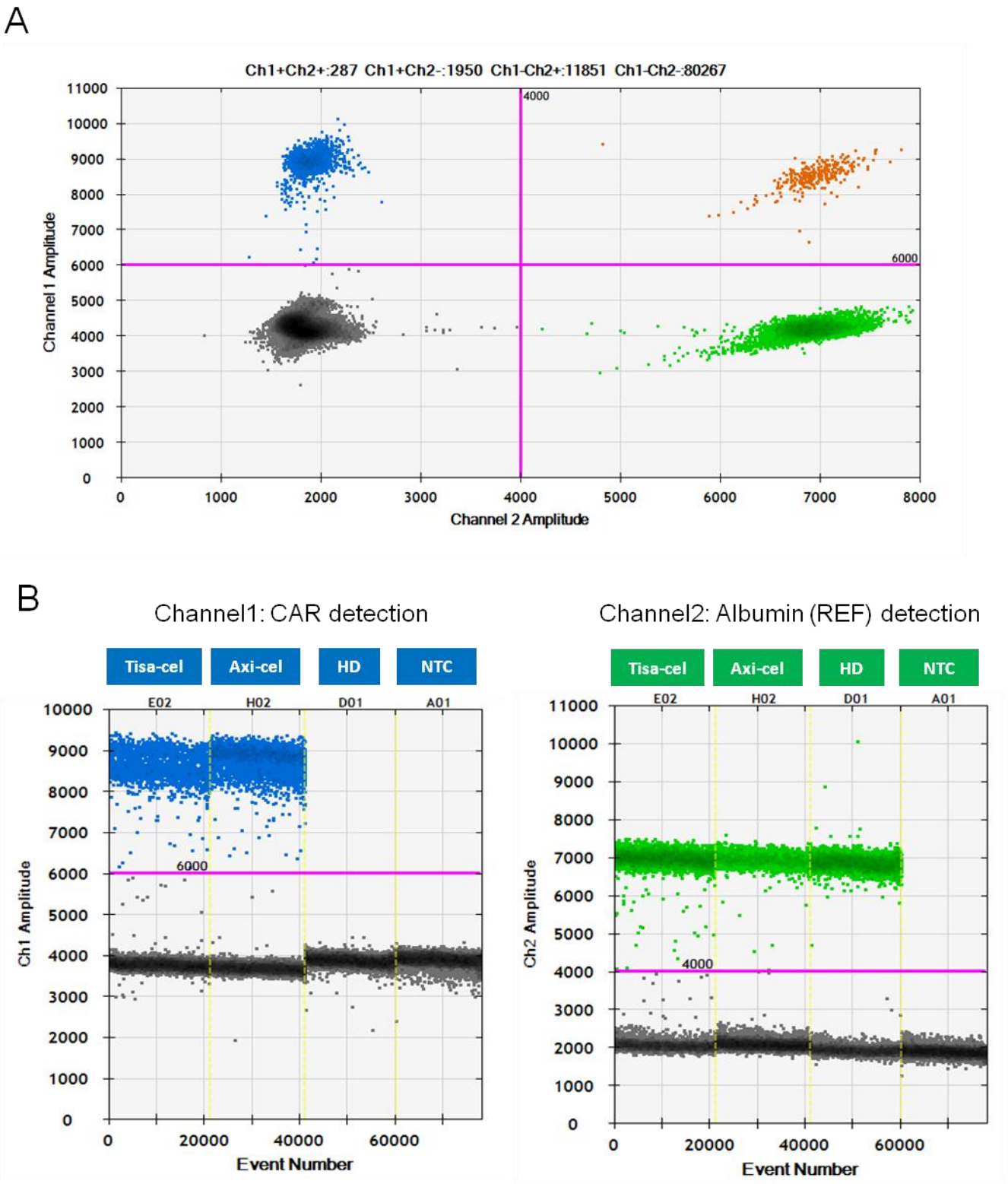

Supplementary Figure 5: Feasibility of the CD19-CAR droplet digital PCR (ddPCR) assay.
A) 2-D visualization plot of ddPCR data outputs. Channel 1 fluorescence (FAM, CAR) is plotted against channel 2 fluorescence (HEX, albumin) for each droplet. As the DNA distribution into droplets follows a random distribution, droplets cluster into four groups: blue dots represent CAR-positive droplets; green dots represent albumin-positive droplets; orange dots represent double-positive droplets; gray dots represent double-negative droplets. **B)** Exemplificative 1-D plot visualization of droplet fluorescence in CAR-positive (tisa-cel and axi-cel) and CAR-negative samples (Healthy Donors, HD, and Non-Template Control, NTC). Each droplet is plotted on fluorescence intensity (y axis) versus droplet number (x axis). All the droplets above the pink threshold line are scored as positive for either CAR (channel 1) or Albumin (channel 2) and all droplets below the pink line are scored as negative.

Supplementary Figure 6

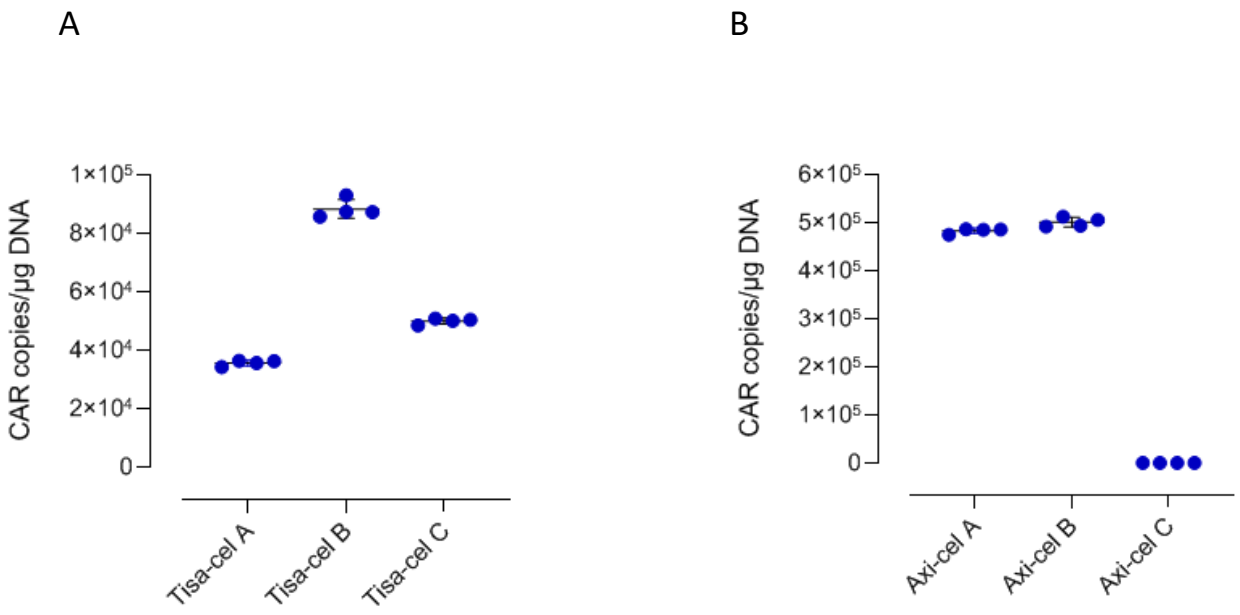

Supplementary Figure 6: Reproducibility of the CD19-CAR droplet digital PCR (ddPCR) assay.
Genomic DNA (gDNA) from 3 infusion bag leftovers of tisa-cel **(A)** and axi-cel **(B)** products were analyzed in quadruplicate in independent ddPCR runs for CAR vector copy counts in order to assess the reproducibility of the ddPCR assay.

Supplementary Figure 7

A

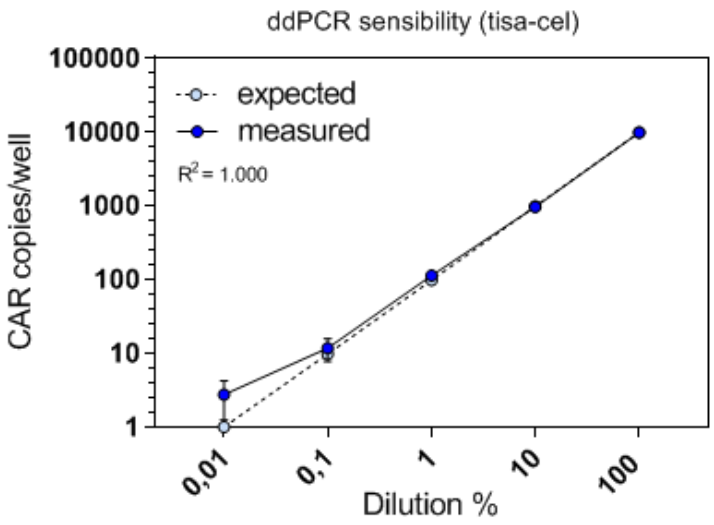

B

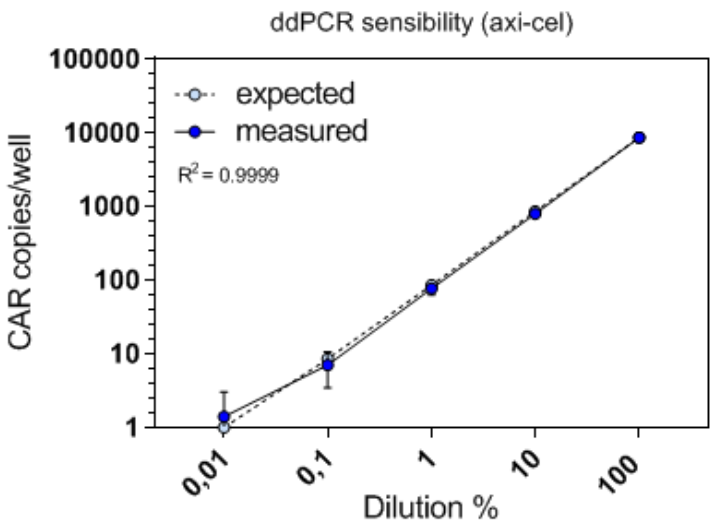

Supplementary Figure 7: Sensibility of the CD19-CAR droplet digital PCR (ddPCR) assay. Serial 1:10 dilutions of 10000 tisa-cel **(A)** and axi-cel CAR vectors **(B)** spiked into 66 ng of genomic DNA (gDNA). Each dilution was performed in gDNA from healthy donors in order to maintain the total amount of 66 ng and dilute just CAR vectors. The experiment resulted in a highly significant linear correlation between measured and expected values, with a slight over-estimation in the lowest dilution, for both products; R^2=0.9994 for tisa-cel and R^2=0.9927 for axi-cel, $P < 0.0001$. Each value is the mean of three replicates. Since the last dilution was expected to contain approximately 1 CAR copy, the assay showed a limit of detection of 1 copy in a background of 10000 cells (as 66ng of gDNA correspond to ca. 10000 equivalent genomes).

Supplementary Figure 8

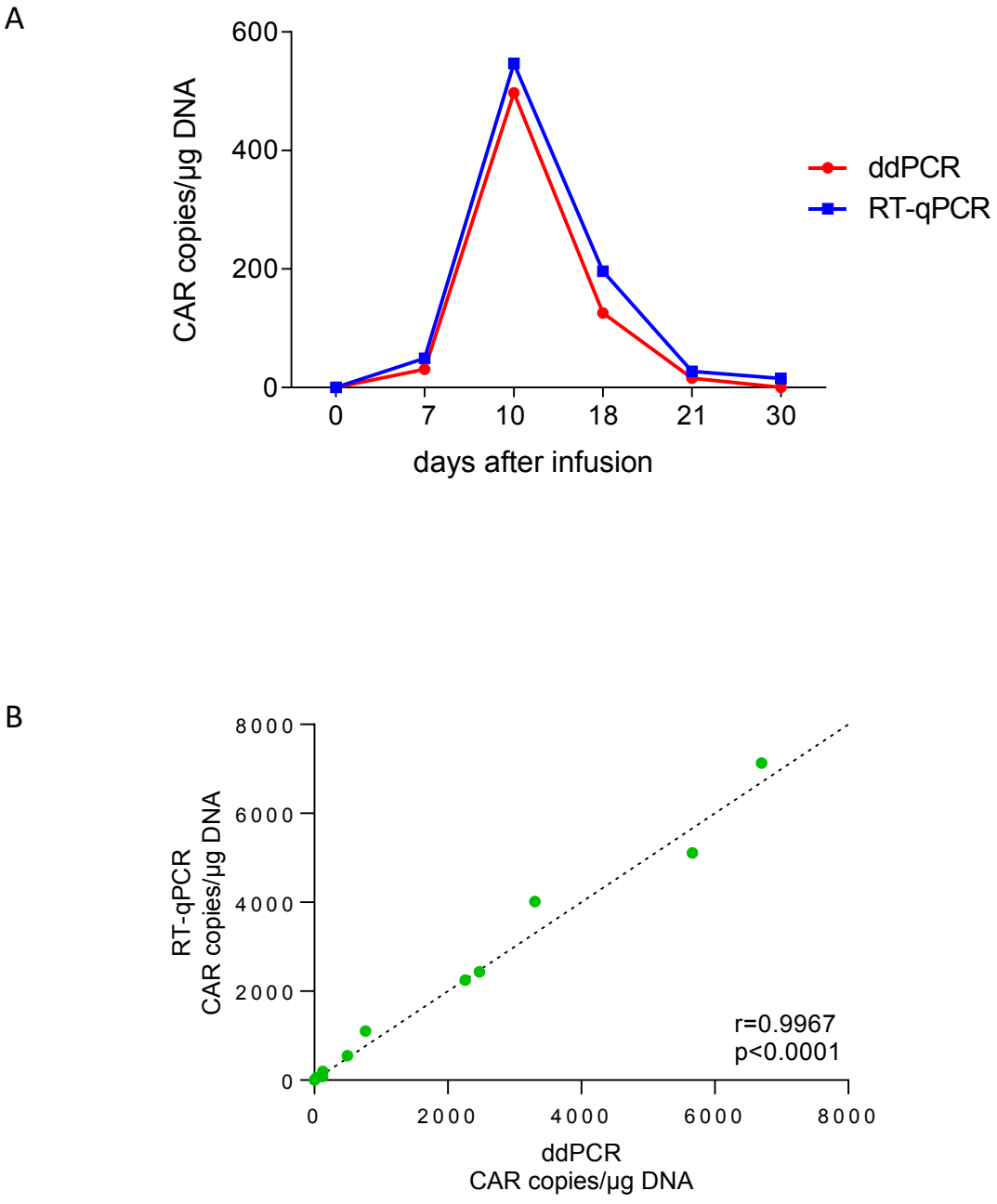

Supplementary Figure 8: Applicability of the in house CD19-CAR assay to reverse transcription quantitative real-time PCR (RT-qPCR).
A) Representative CAR T expansion kinetics evaluated using the in-house set of primers-probe for droplet digital PCR (ddPCR) (red line) and RT-qPCR (blue line) experiments. **B)** Scatter dot plots showing the Spearman correlation between CAR copies/µg DNA obtained by ddPCR and RT-qPCR.

Supplementary Figure 9

A

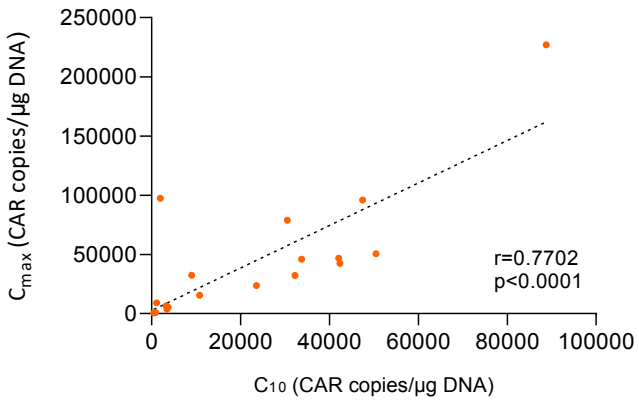

B

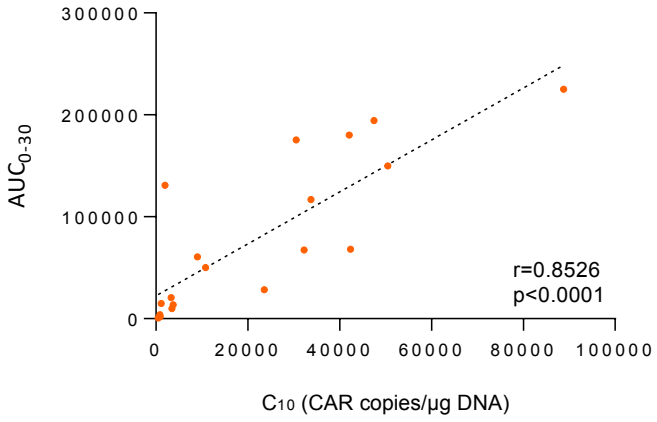

C

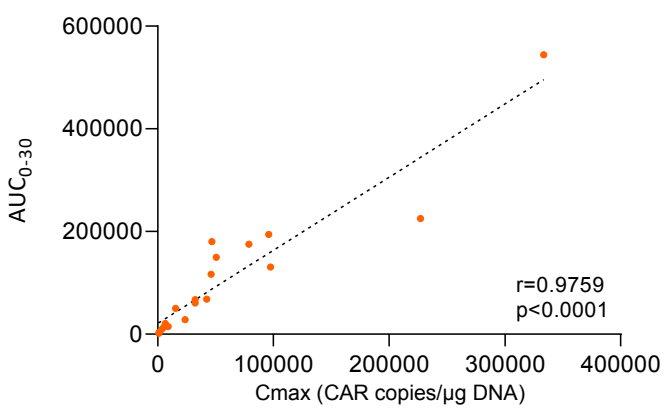

Supplementary Figure 9: Kinetic parameters evaluated by droplet digital PCR (ddPCR) were strongly correlated.

Scatter dot plots showing the Spearman correlations between: **A)** CAR T count at day 10 post-infusion (C_{10}) and at peak expansion (C_{max}) (n=167); **B)** CAR T count at day 10 post-infusion (C_{10}) and median cumulative CAR T level within the first month (AUC_{0-30}) (n=167); **C)** CAR T count at peak expansion (C_{max}) and median cumulative CAR T level within the first month (AUC_{0-30}) (n=20).

Supplementary Figure 10

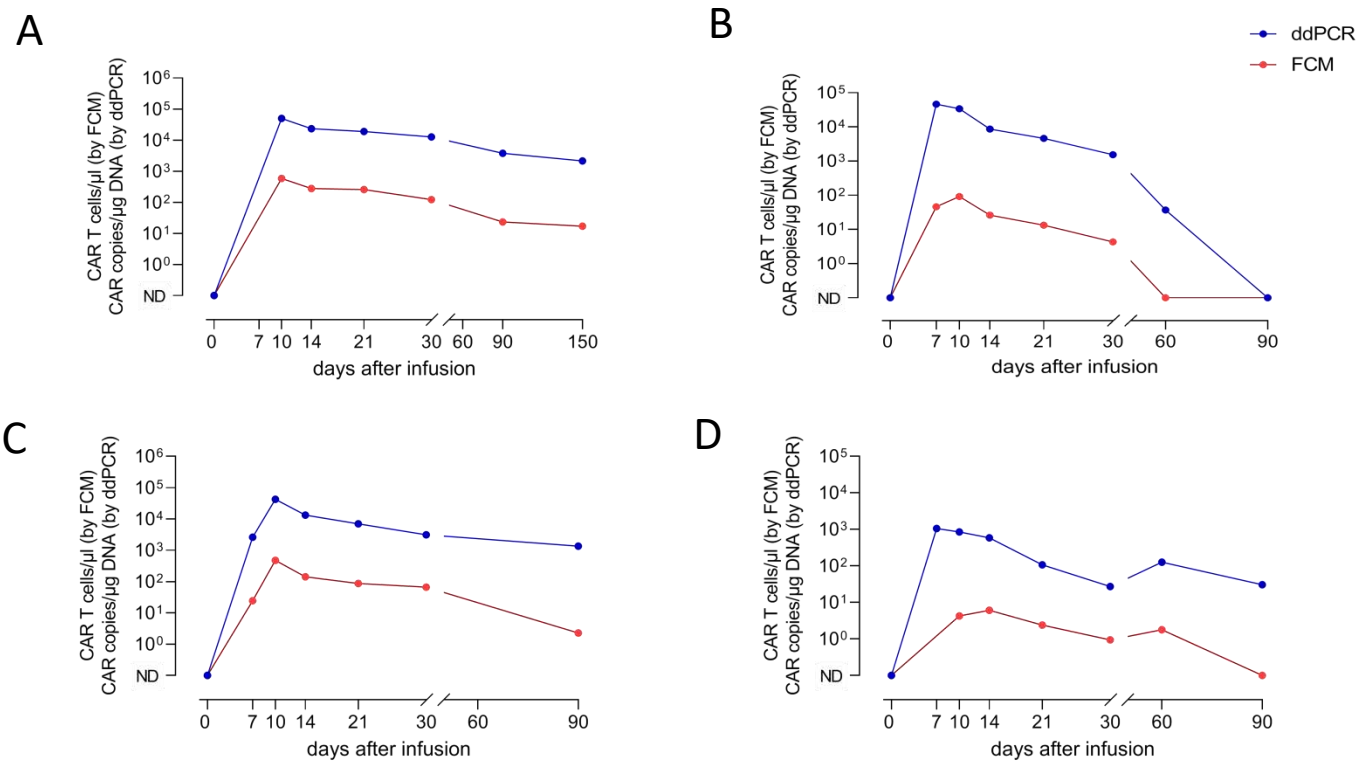

Supplementary Figure 10: Exemplificative longitudinal CAR T expansion kinetics assessed by flow cytometry (FCM) and droplet digital PCR (ddPCR).

A-D) Representative examples of expansion kinetics evaluated by FCM and ddPCR: the two techniques gave similar trends for the entire monitoring.

Supplementary Figure 11

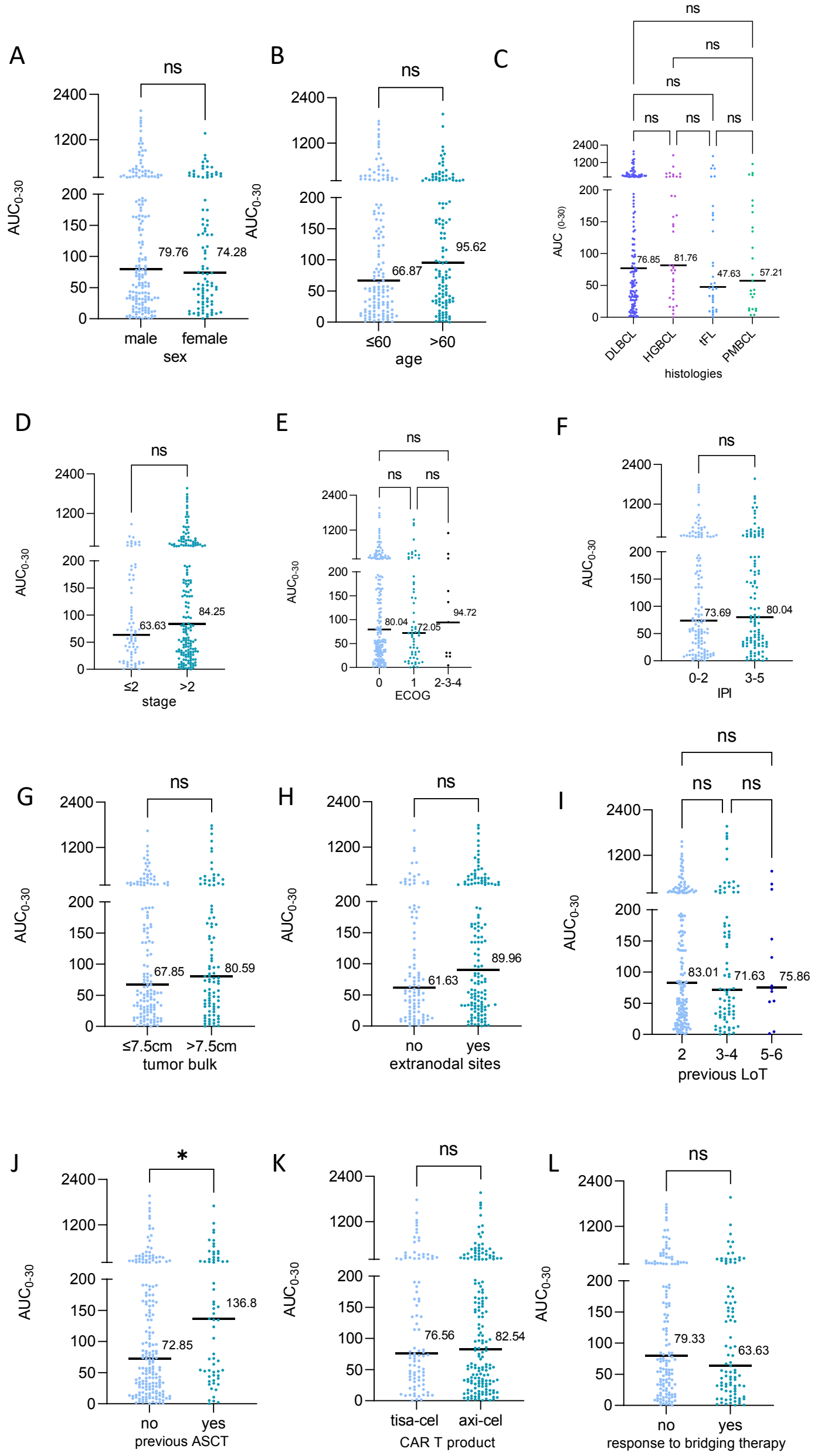

Supplementary Figure 11

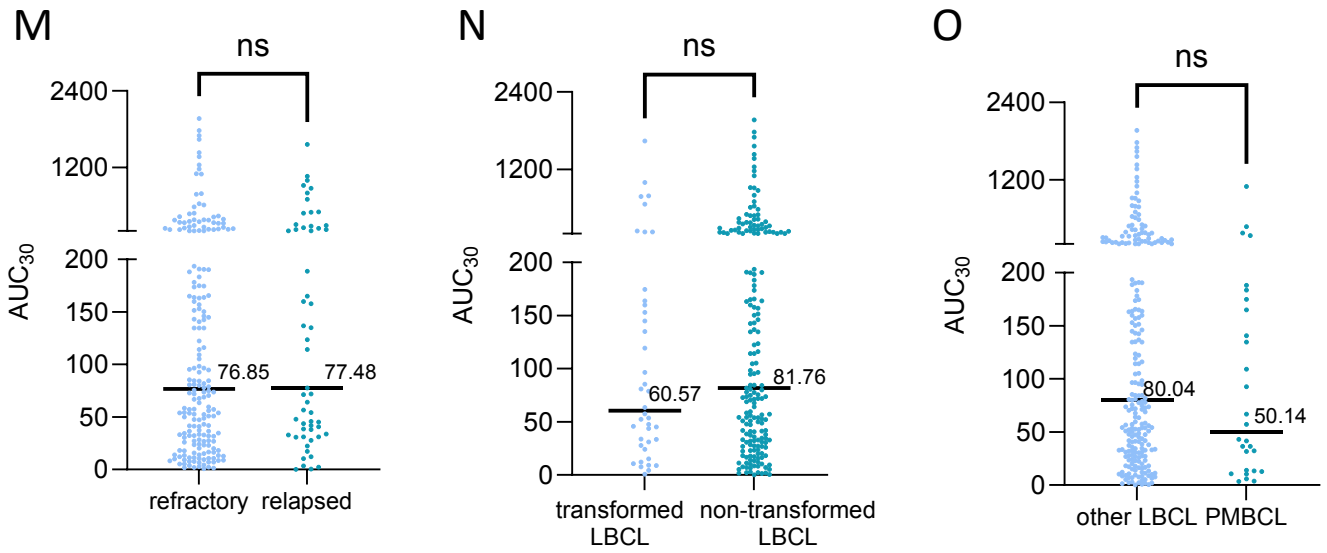

Supplementary Figure 11: CAR T expansion in relation to patients' characteristics.
CAR T expansion within the first month after infusion ($AUC_{0\text{-}30}$) stratified by sex **(A)**, age **(B)**, disease histotype (DLBCL: Diffuse Large B-cell Lymphoma; HGBCL: High Grade B-cell Lymphoma; PMBCL: Primary Mediastinal B-cell Lymphoma; tFL: transformed Follicular Lymphoma) **(C)**, stage at leukapheresis **(D)**, Eastern Cooperative Oncology Group (ECOG) **(E)**, international prognostic index (IPI) score **(F)**, tumor bulk **(G)**, presence of extranodal sites **(H),** previous lines of therapy (LoT) **(I)**, previous autologous stem cell transplant (ASCT) **(J)**, CAR T product received **(K)**, response to bridging therapy **(L)**, disease status **(M)**, large B-cell lymphoma (LBCL) subtype **(N-O)**. N=262. Exact median values are reported. *P* values were calculated applying the Mann–Whitney test; ns=not significant, * *P*<0.05.

Supplementary Figure 12

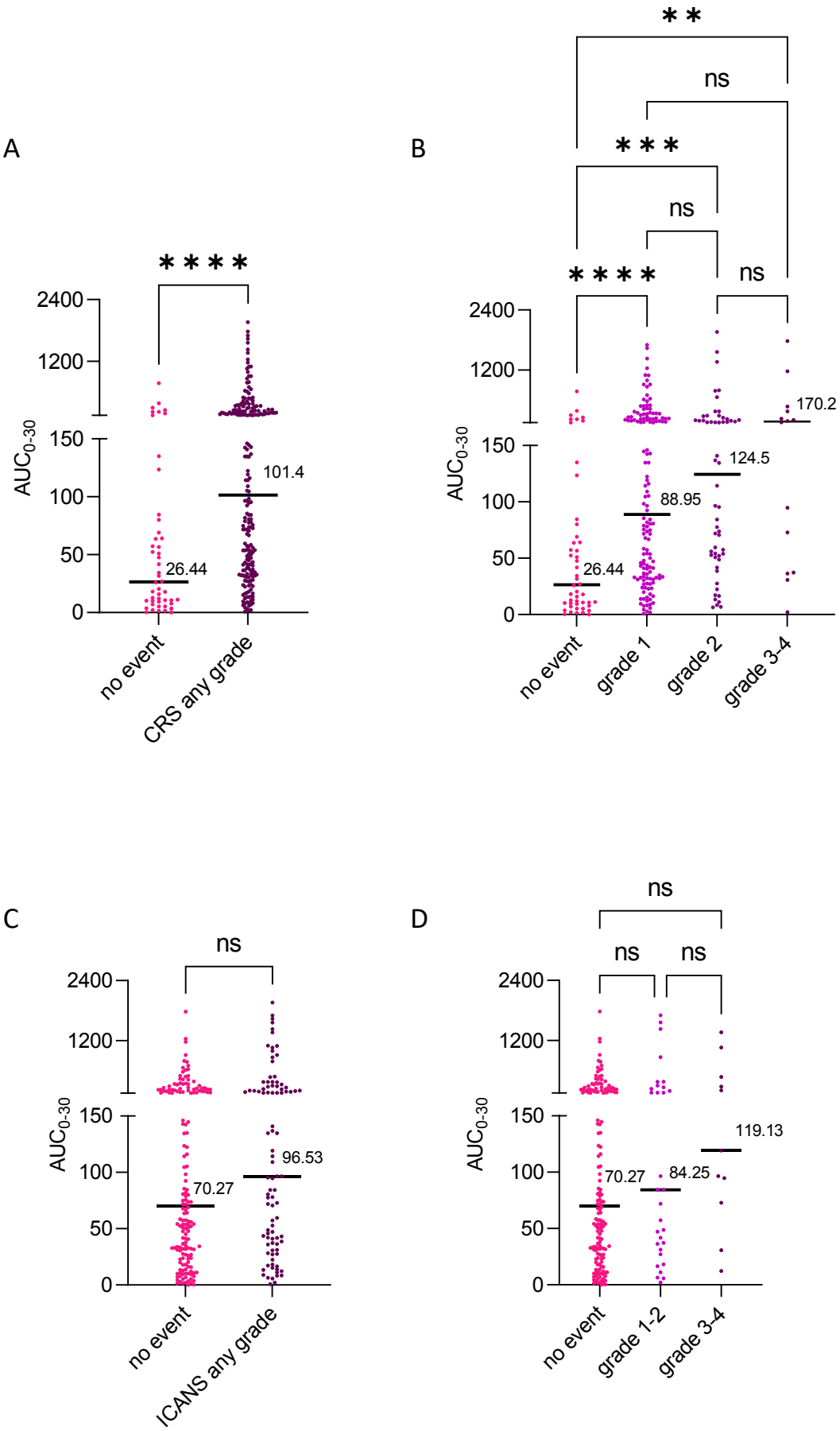

Supplementary Figure 12: CAR T expansion in relation to Cytokine release syndrome (CRS) and Immune effector cell-associated neurotoxicity syndrome (ICANS).
CRS was observed in the majority of patients (n=214, 81.7%), primarily grade 1 (n=142, 66.3%). ICANS occurred in 94 patients (36%). CAR T expansion within the first month after infusion (AUC_{0-30}) stratified by CRS occurrence (n=262) **(A)**, CRS grade (n=262) **(B)**, ICANS occurrence (n=262) **(C)** and ICANS grade (n=262) **(D)**. Exact median values are reported. *P* values were calculated applying the Mann–Whitney test; ns=not significant, ** *P*<0.01, *** *P*<0.001, **** *P*<0.0001.

Supplementary Figure 13

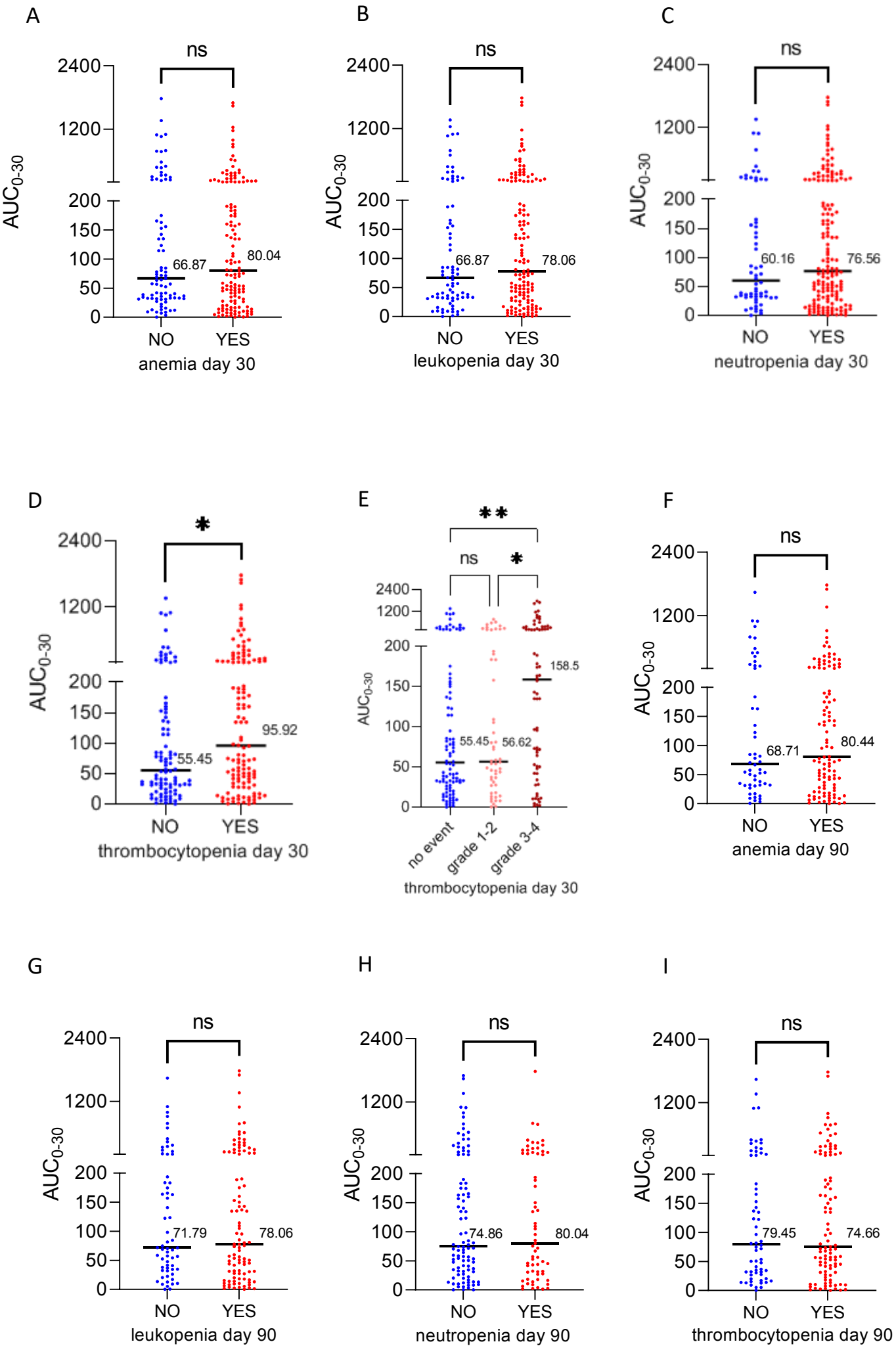

Supplementary Figure 13: CAR T expansion in relation to hematological toxicities.
CAR T expansion within the first month after infusion (AUC_{0-30}) stratified by: day 30 anemia (n=220) **(A)**, day 30 leukopenia (n=220) **(B),** day 30 neutropenia (n=220) **(C)**, day 30 thrombocytopenia (n=220) **(D** and **E)**, day 90 anemia (n=164) **(F)**, day 90 leukopenia (n=164) **(G),** day 90 neutropenia (n=164) **(H),** and day 90 thrombocytopenia (n=164) **(I)**. Exact median values are reported. *P* values were calculated applying the Mann–Whitney test; ns=not significant, * $P<0.05$, ** $P<0.01$.

Supplementary Figure 14

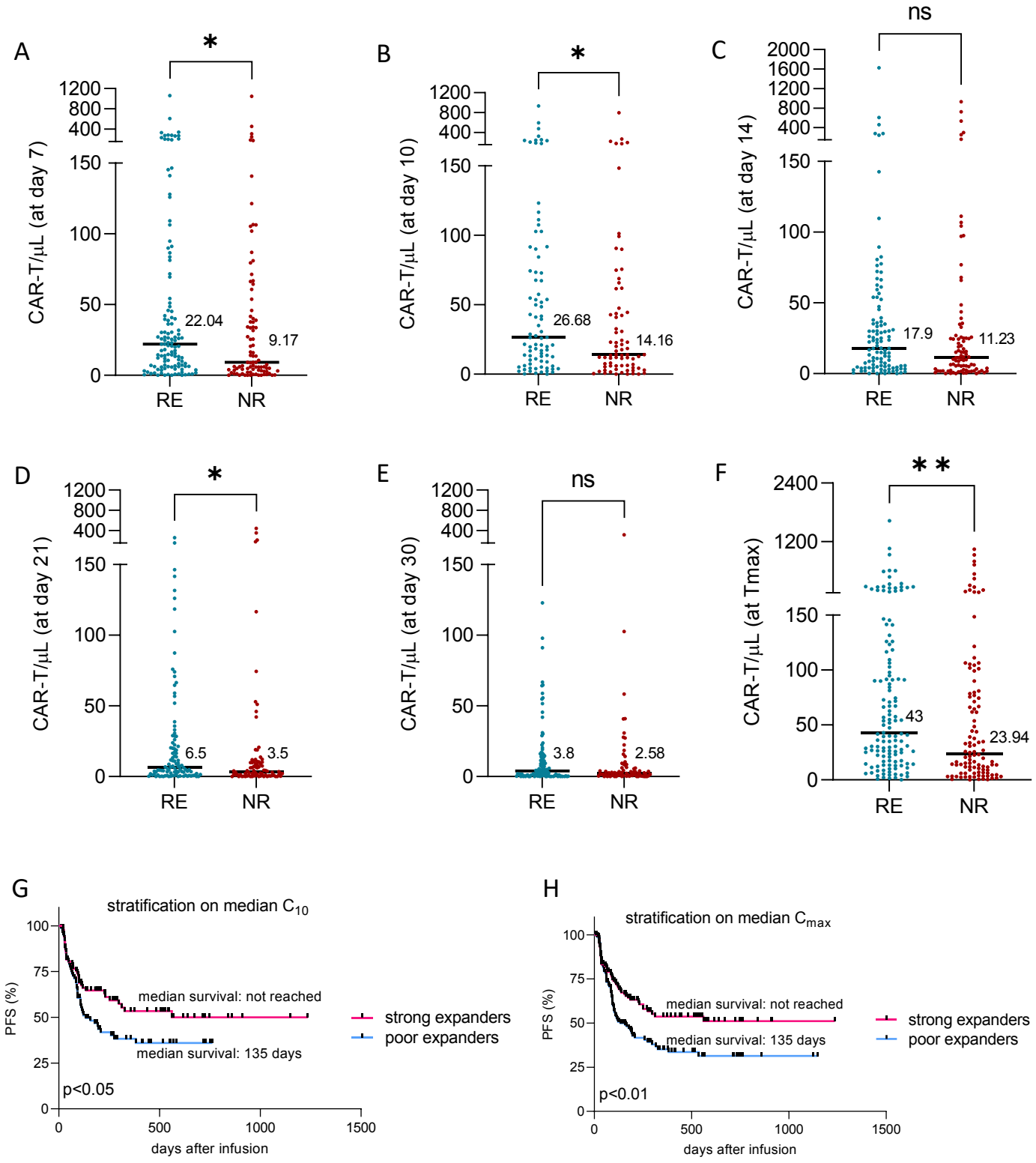

Supplementary Figure 14: CAR T expansion is positively associated with day 90 response and progression-free survival (PFS).

A) CAR T-cell counts at day 7 after infusion in responder (RE) and non-responder patients (NR) patients by day 90 (n=211). **B)** CAR T-cell counts at day 10 after infusion (C_{10}) in RE and NR patients by day 90 (n=156). **C)** CAR T-cell counts at day 14 after infusion in RE and NR patients by day 90 (n=196). **D)** CAR T-cell counts at day 21 after infusion in RE and NR patients by day 90 (n=181). **E)** CAR T-cell counts at day 30 after infusion in RE and NR patients by day 90 (n=191). **F)** CAR T-cell counts at peak expansion (T_{max}) in RE and NR by day 90 (n=235). In A-H, exact median values are reported. *P* values were calculated applying the Mann–Whitney test; ns=not significant, * $P<0.05$, ** $P<0.01$.

G) Kaplan–Meier curve showing PFS according to CAR T-cell expansion (n=167). Patients were dichotomized into strong and poor expanders based on the median CAR T counts at day 10 (C_{10}). **H)** Kaplan–Meier curve showing PFS according to CAR T-cell expansion (n=262). Patients were dichotomized into strong and poor expanders based on the median CAR T counts at peak expansion (C_{max}). In G-H, comparisons were made applying the log-rank test.

Supplementary Figure 15

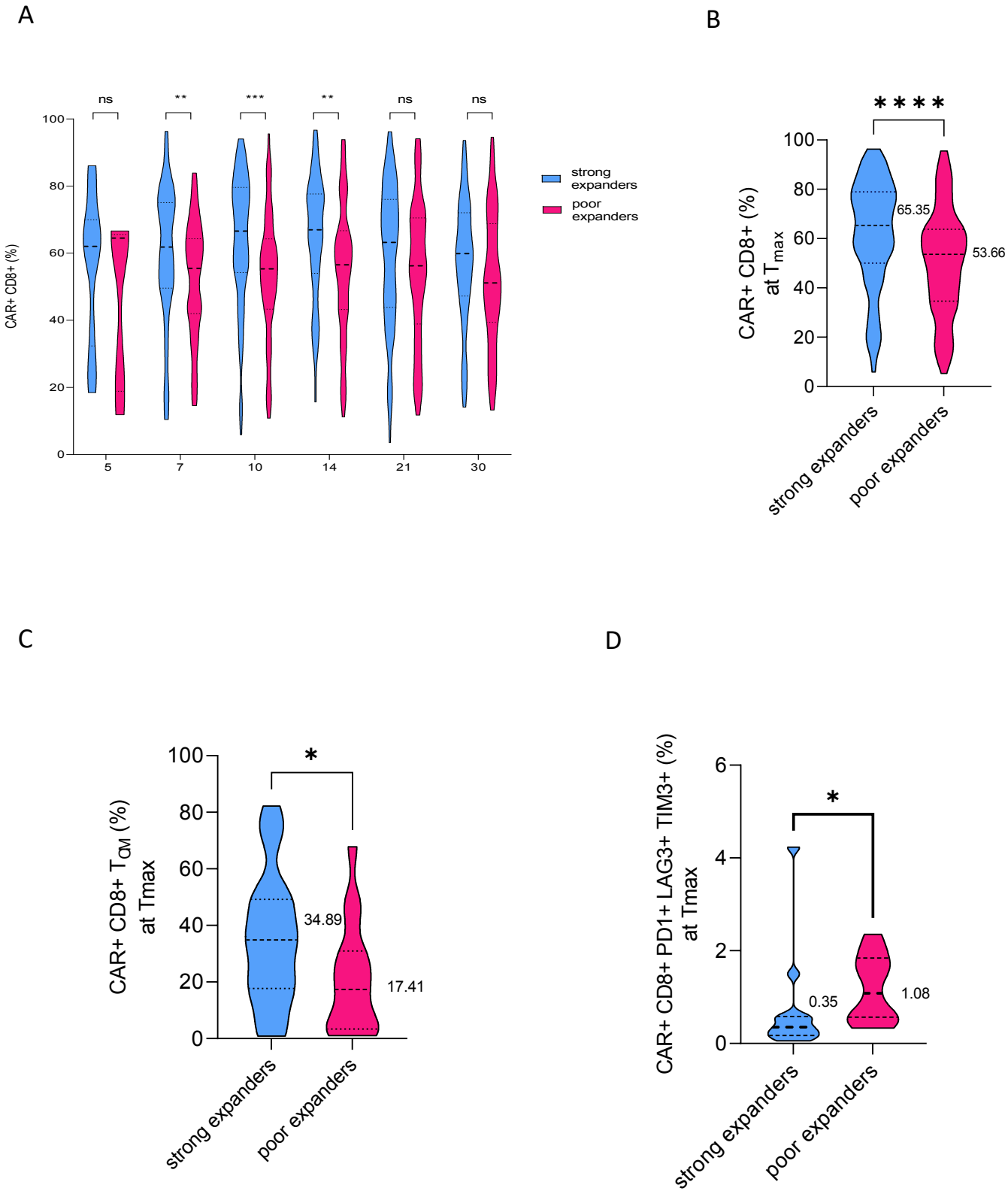

Supplementary Figure 15: CAR+CD8+ cells with a more immature and less exhausted phenotype are significantly higher in strong expanders.
A) and **B)** Graphs showing the % of CAR+CD8+ cells at the indicated time points after infusion, in expander and poor expander patients [dichotomized based on the median CAR T expansion within the first month after infusion ($AUC_{0\text{-}30}$)] (n=262). **C)** Levels of CAR+CD8+ T central memory (T_{CM}) cells at peak expansion (T_{max}), in expander and poor expander patients (dichotomized based on the median $AUC_{0\text{-}30}$) (n=43). **D)** Levels of exhausted CAR+CD8+ cells at peak expansion (T_{max}), in expander and poor expander patients (dichotomized based on the median $AUC_{0\text{-}30}$) (n=23). Exact median values are reported. *P* values were calculated applying the Mann–Whitney test; ns=not significant, * $P<0.05$, ** $P<0.01$, *** $P<0.001$; **** $P<0.0001$.

Supplementary Figure 16

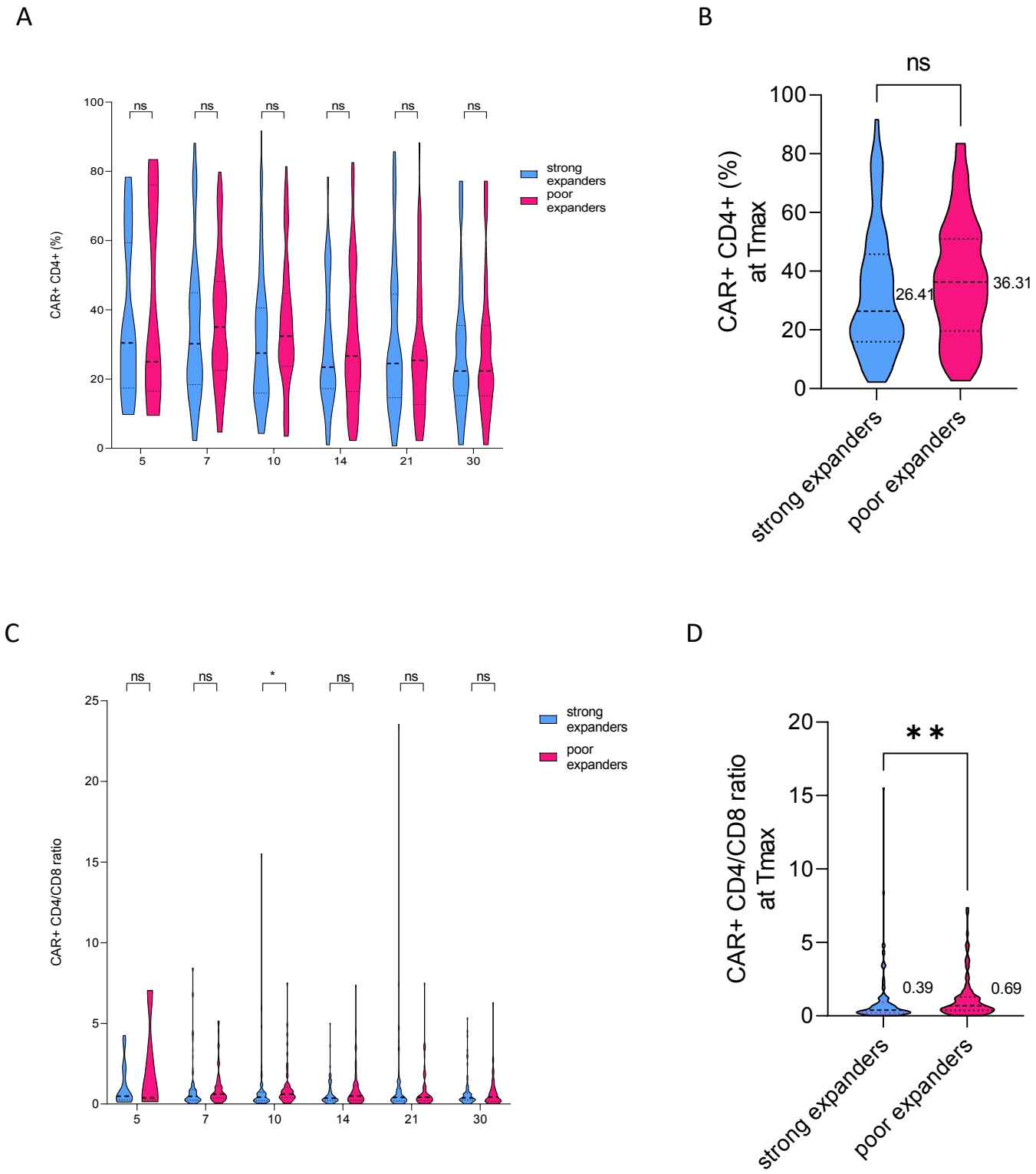

Supplementary Figure 16: Differences in CAR+CD4+ and CAR+CD4/CD8 ratio between strong and poor expanders.

A) and **B)** Graphs showing the % of CAR+CD4+ cells at the indicated time points after infusion, in expander and poor expander patients [dichotomized based on the median CAR T expansion within the first month after infusion ($AUC_{0\text{-}30}$)] (n=262). **C)** and **D)** Graph showing the CAR+ CD4/CD8 ratio at the indicated time-points after infusion, in expander and poor expander patients (dichotomized based on the median $AUC_{0\text{-}30}$) (n=262). T_{max}: peak expansion. Exact median values are reported. *P* values were calculated applying the Mann–Whitney test; ns=not significant, * $P<0.05$, ** $P<0.01$.

Supplementary Figure 17

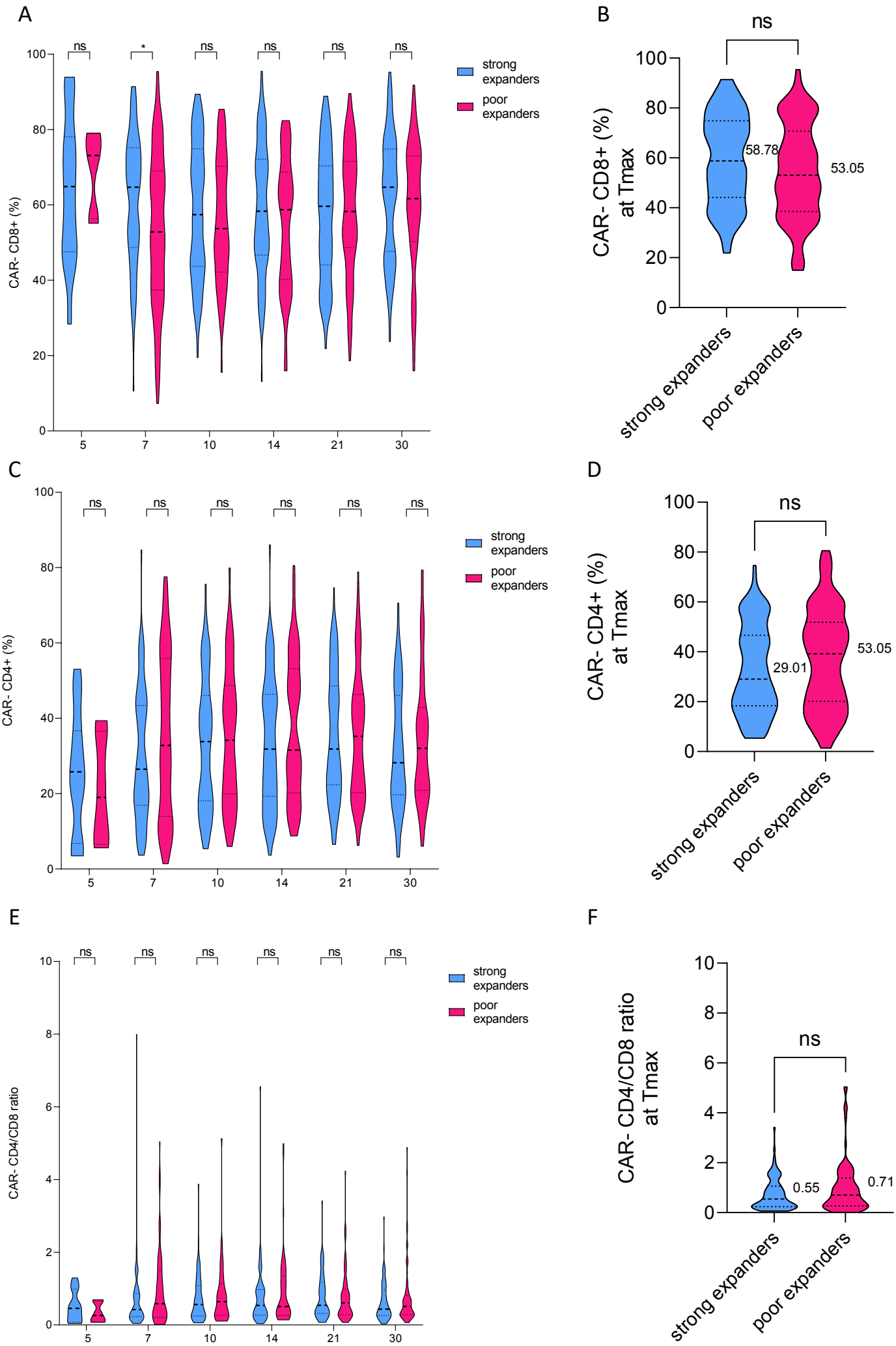

Supplementary Figure 17: Differences in CAR-CD8+, CAR-CD4+ and CAR-CD4/CD8 ratio between strong and poor expanders.

A) and **B)** Graph showing the % of CAR-CD8+ cells at the indicated time points after infusion, in expander and poor expander patients. **C)** and **D)** Graph showing the % of CAR-CD4+ cells at the indicated time-points after infusion, in expander and poor expander patients. **E)** and **F)** Graph showing the CAR-CD4/CD8 ratio at the indicated time-points after infusion, in expander and poor expander patients. A-F: patients were dichotomized based on the median CAR T expansion within the first month after infusion ($AUC_{0\text{-}30}$) (n=262). T_{max}: peak expansion. Exact median values are reported. *P* values were calculated applying the Mann–Whitney test; ns=not significant, * *P*<0.05.

Supplementary Figure 18

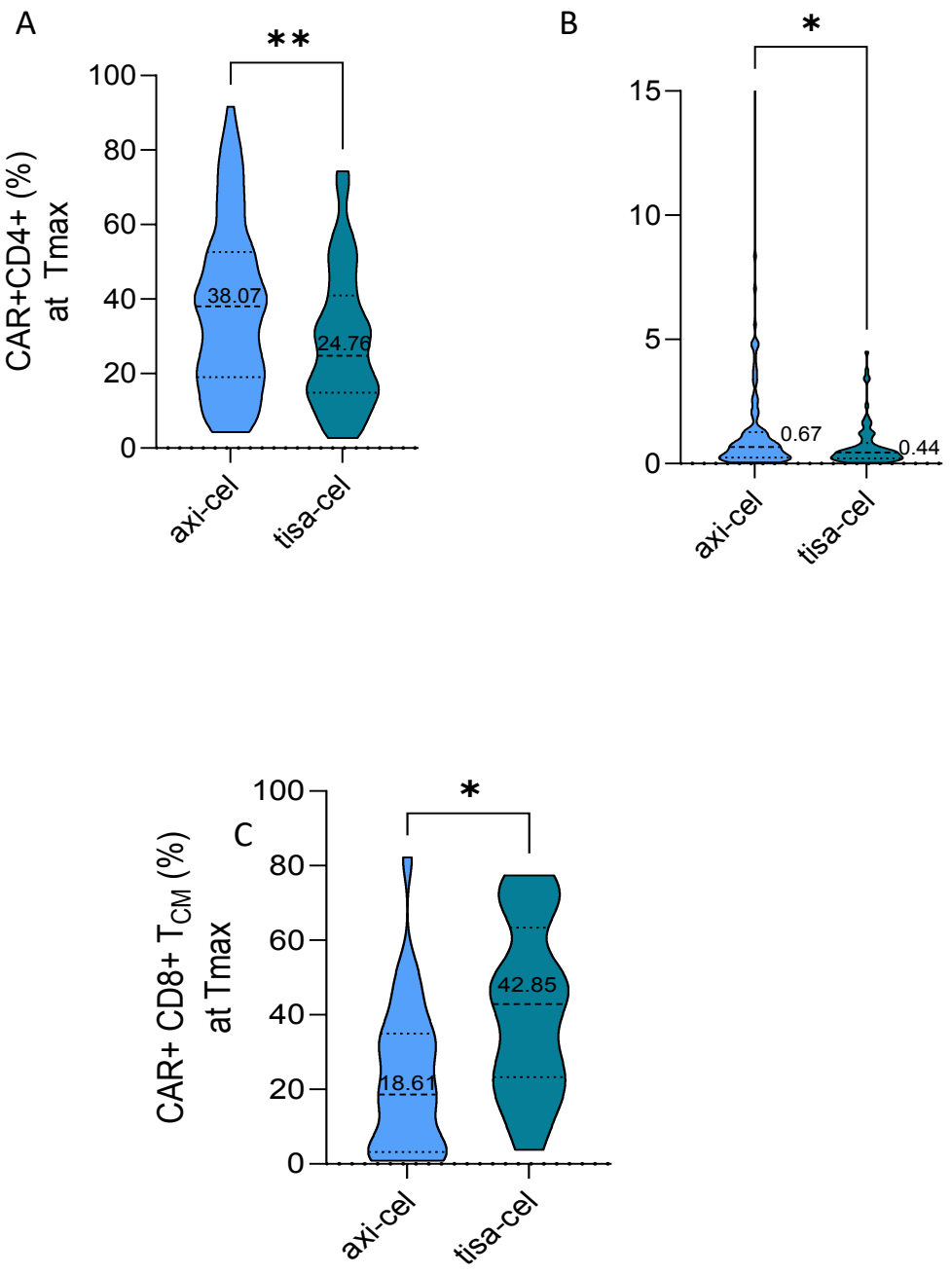

Supplementary Figure 18: Differences in CAR+ populations between axi-cel and tisa-cel at peak expansion (T_{max}).
A) Graph showing the % of CAR+CD4+ cells at the T_{max} in axi-cel and tisa-cel treated patients. **B)** Graph showing the % of CAR+CD4/CD8 ratio at the T_{max} in axi-cel and tisa-cel treated patients. **C)** Graph showing the % of CAR+CD8+ central memory T cells (T_{CM}) at the T_{max} in axi-cel and tisa-cel treated patients. Exact median values are reported. *P* values were calculated applying the Mann–Whitney test; ns=not significant, * *P*<0.05.

.

Supplementary Figure 19

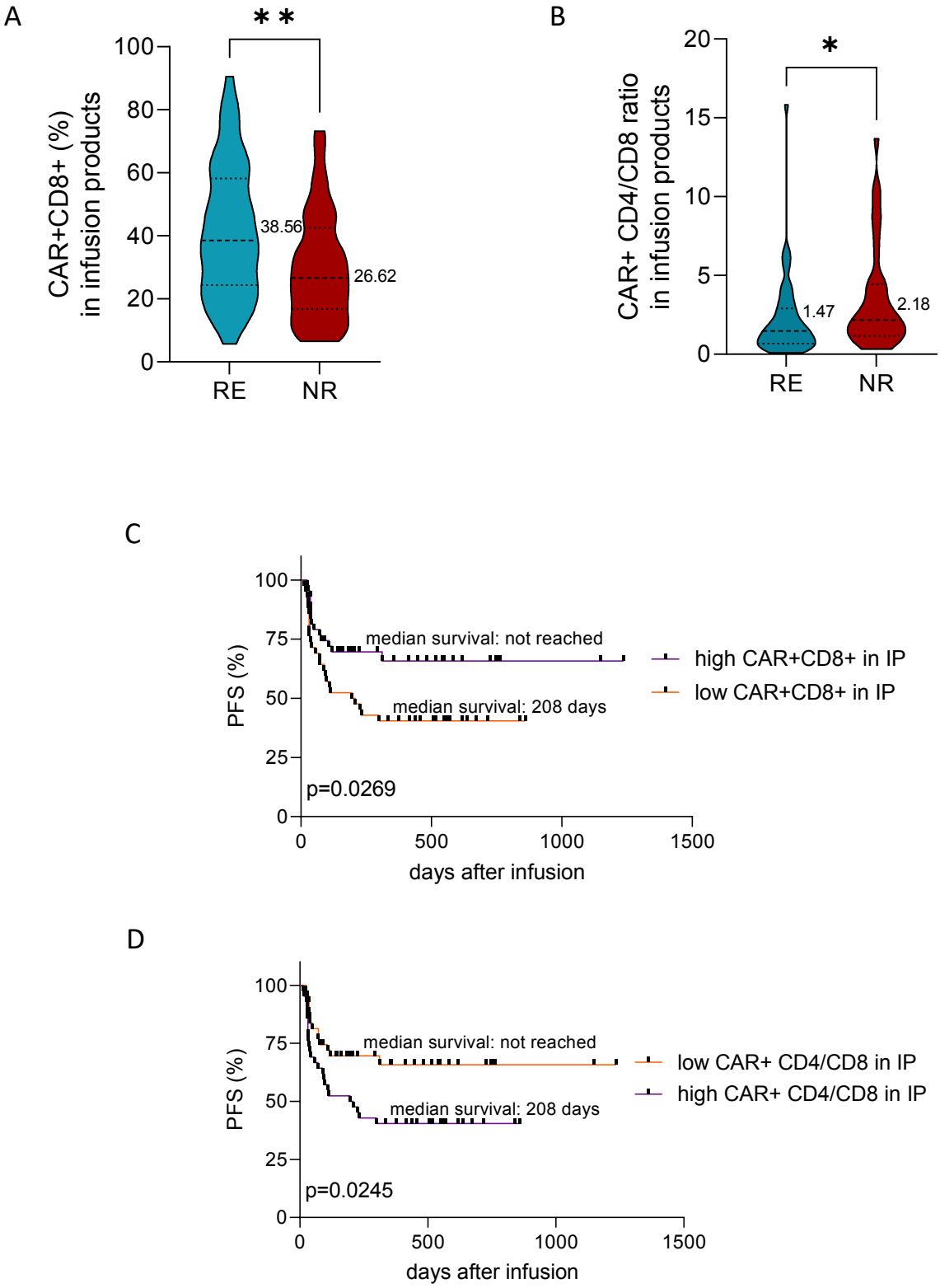

Supplementary Figure 19: The levels CAR+CD8+ and CAR+CD4/CD8 ratio in infusion products significantly impact day 90 response and progression-free survival (PFS).

A-B) Graphs showing the levels of CAR+CD8+ cells and the CAR+CD4/CD8 ratio in infusion products (IP) , in responder (RE) and non responder (NR) patients by day 90 (n=86). Exact median values are reported. *P* values were calculated applying the Mann–Whitney test; * *P*<0.05, ** *P*<0.01.

C-D) Kaplan-Meier curves of PFS in patients stratified according to the levels of CAR+CD8+ cells and the CAR+CD4/CD8 ratio in infusion products (IP) (n=86). The cut-off used to dichotomize patients was the median value (34% for CAR+CD8+ levels, 1.84 for CAR+CD4/CD8 ratio). Comparison was made applying the log-rank test.

Supplementary Figure 20

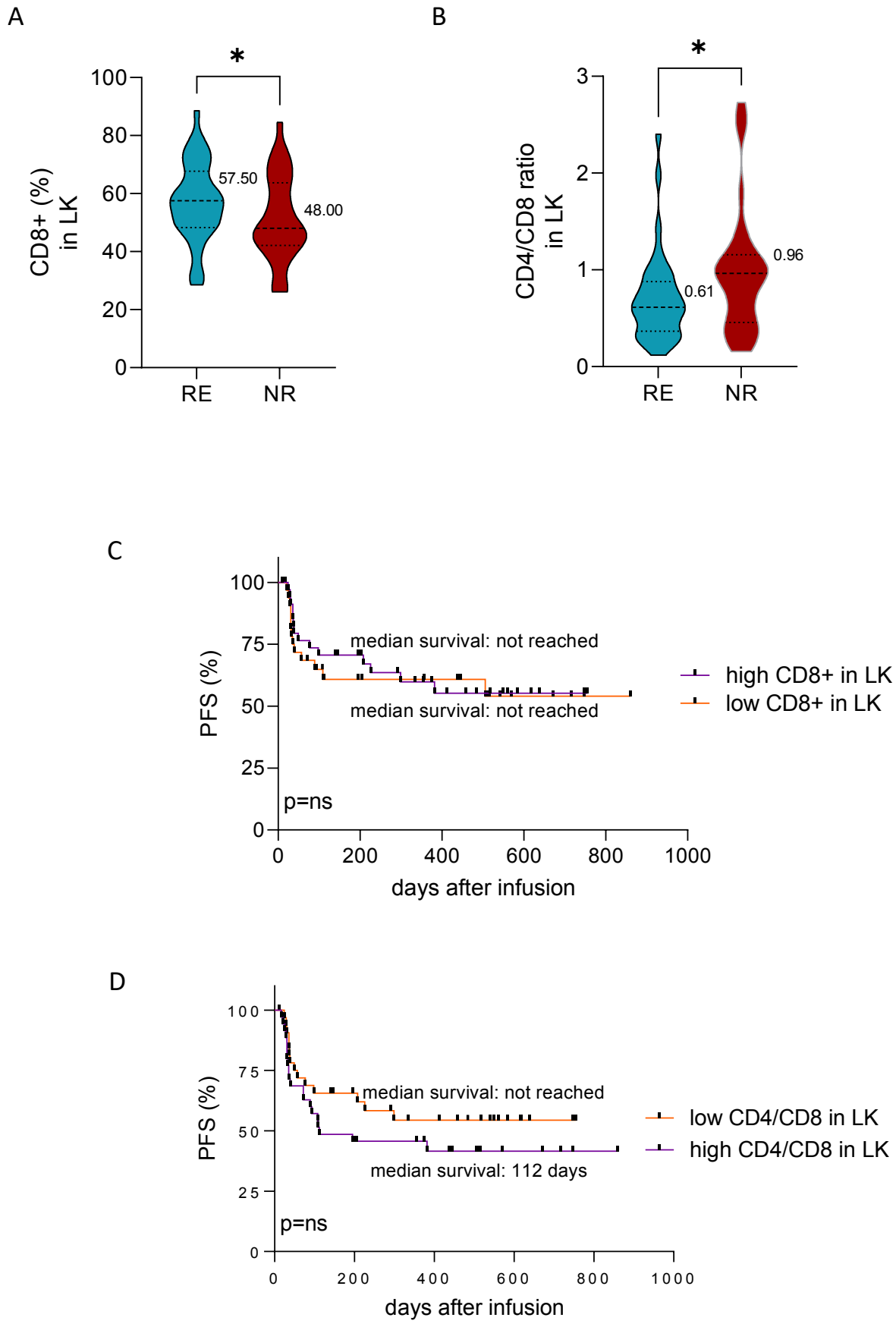

Supplementary Figure 20: The levels of CD8+ and CD4/CD8 ratio in leukapheresis (LK) products significantly impact day 90 response.

A-B) Graphs showing the levels of CD8+ cells and the CD4/CD8 ratio in LK products, in responder (RE) and non responder (NR) patients by day 90 (n=67). Exact median values are reported. *P* values were calculated applying the Mann–Whitney test; * *P*<0.05.

C-D) Kaplan-Meier curves of progression-free survival (PFS) in patients stratified according to the levels of CD8+ cells and the CD4/CD8 ratio in LK products (n=67). The cut-off used to dichotomize patients was the median value (53.5% for CD8+ levels, 0.73 for CD4/CD8 ratio). Comparison was made applying the log-rank test.

Supplementary Figure 21

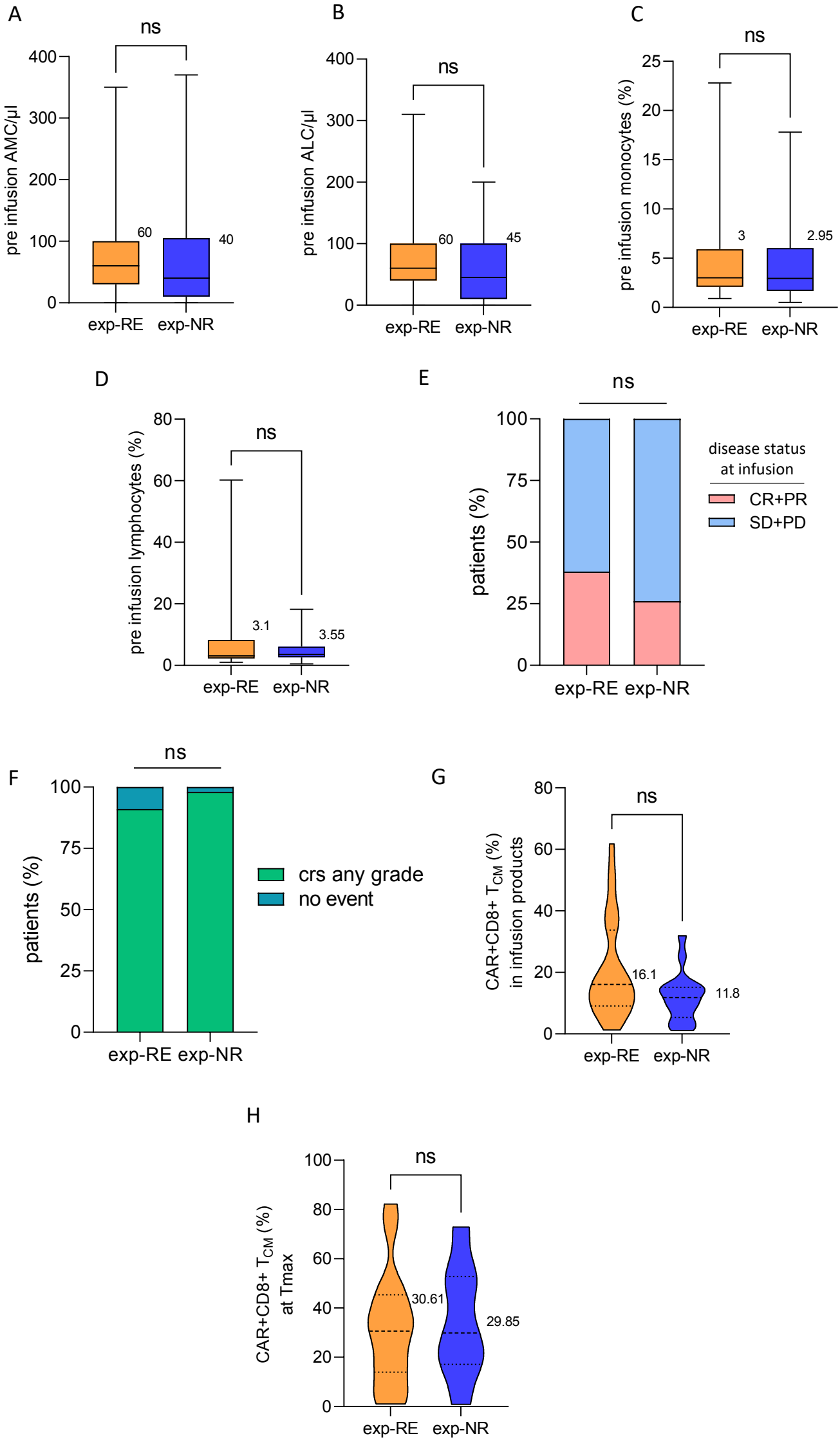

Supplementary Figure 21: Analysis of clinical and biological features at infusion in expanders who responded (exp-RE) and expanders who did not respond (exp-NR) by day 90 .

Graphs showing pre infusion values of absolute monocyte counts (AMC) **(A)**, absolute lymphocyte counts (ALC) **(B)**, % of monocyte **(C),** and % of lymphocytes **(D)** in exp-RE and exp-NR (n=53).

E) Bar plot representing how patients are distributed into the different groups analyzed. Patients were dichotomized into exp-RE and exp-NR and the disease status at infusion was considered (CR: complete response, PR: partial response, SD: stable disease, PD: progressive disease). $\chi 2$ test was applied to evaluate statistical significance. **F)** Bar plot representing how patients are distributed into the different groups analyzed. Patients were dichotomized into exp-RE and exp-NR and the occurrence of any grade cytokine release syndrome (CRS) was considered. $\chi 2$ test was applied to evaluate statistical significance. **G)** Levels of CAR+CD8+ T central memory (T_{CM}) cells in infusion products, in exp-RE and exp-NR (n=43). **H)** Levels of T_{CM} cells at peak expansion (T_{max}), in exp-RE and exp-NR (n=32).

In A-D, G and H exact median values are reported. *P* values were calculated applying the Mann–Whitney test; ns=not significant.

Supplementary Figure 22

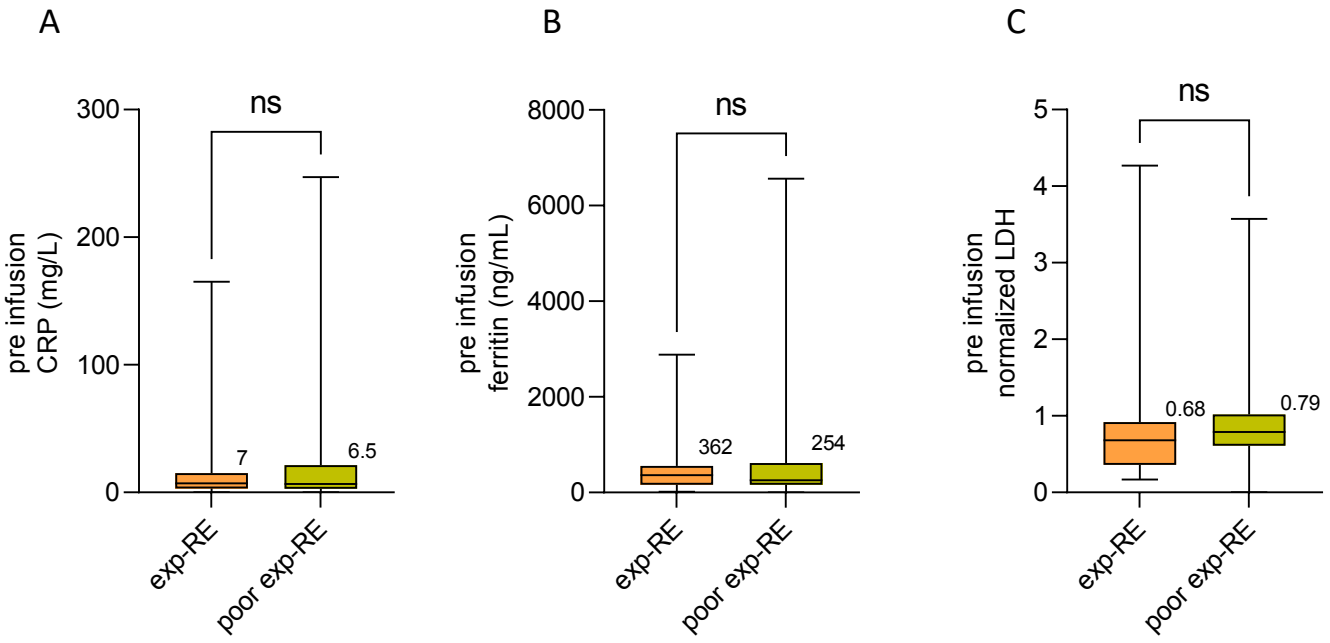

Supplementary Figure 22: Pre infusion levels of C-reactive Protein (CRP), ferritin and normalized lactate dehydrogenase (LDH) in exp-RE and poor exp-RE.
Graphs showing pre infusion values of CRP (n=127) **(A)**, ferritin (n=118) **(B)** and normalized LDH (n=106) **(C)** in expanders who responded (exp-RE) and poor expanders who responded by day 90 (poor exp-RE). LDH levels were divided by the respective upper limit of normal (ULN), to generate normalized ratios. Ratios >1 correspond to LDH levels higher than ULN. Exact median values are reported. *P* values were calculated applying the Mann–Whitney test; ns=not significant.

Supplementary Figure 23

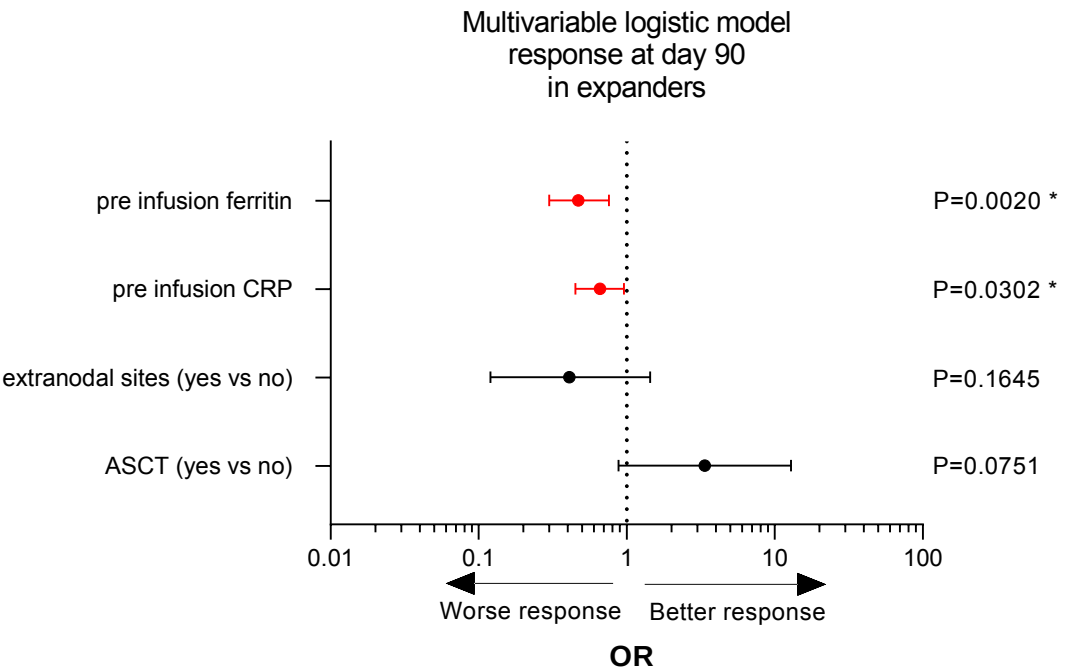

Supplementary Figure 23: Multivariable logistic model for response at day 90 in the subgroup of expander patients.

Forest plot reporting the results of a multivariable logistic model assessing potential risk factors for response at day 90 in expander patients (n=91). CRP: C-reactive protein; ASCT: autologous stem cell transplant; OR: Odds ratio.

Supplementary Figure 24

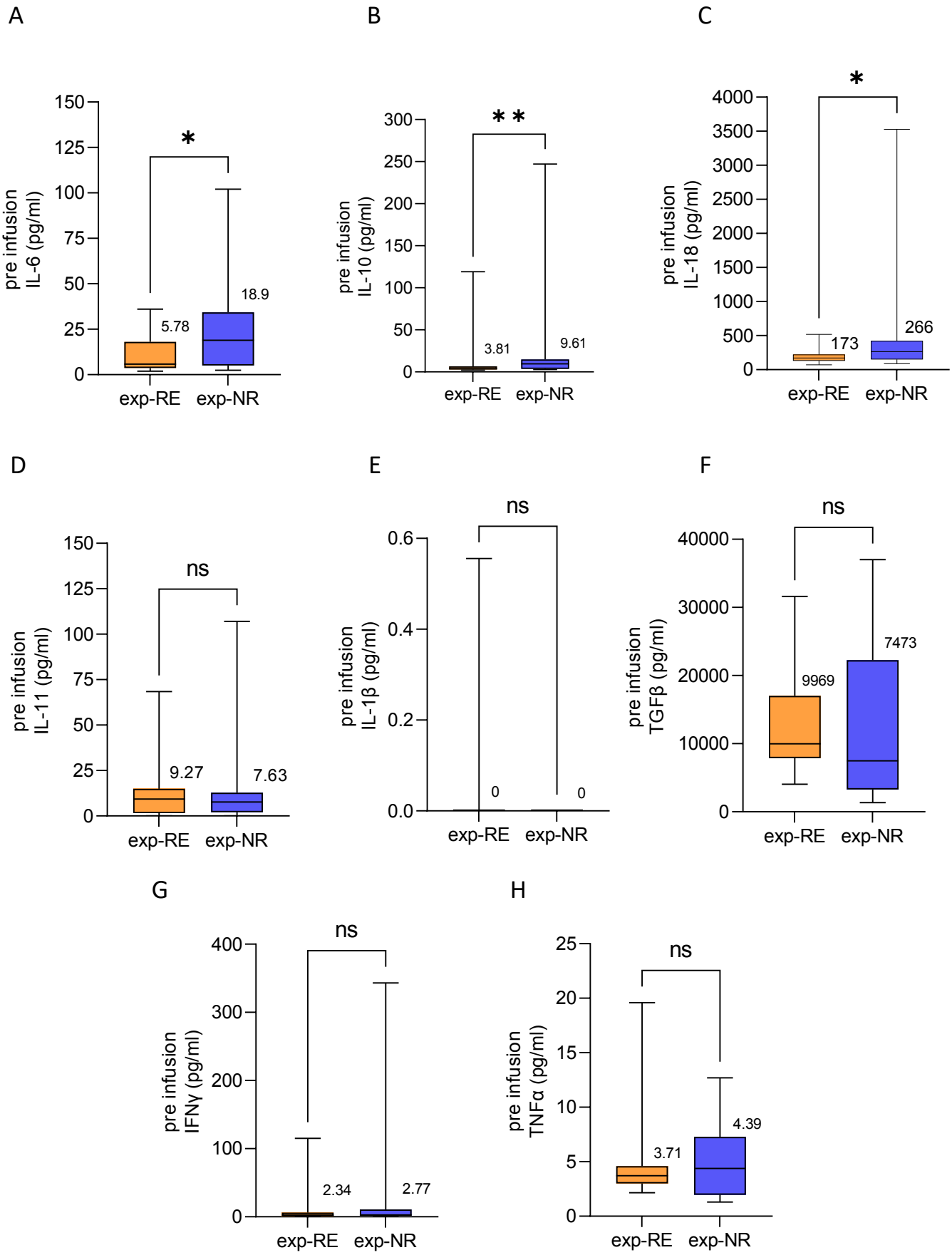

Supplementary Figure 24: Pre infusion levels of pro-inflammatory and anti-inflammatory cytokines in exp-RE and exp-NR.

Graphs showing pre infusion values of IL-6 (n=48) **(A)**, IL-10 (n=39) **(B)**, IL-18 (n=47) **(C),** IL-11 (n=48) **(D),** IL-1β (n=48) **(E)**, TGFβ (n=19) **(F)**, IFNγ (n=48) **(G)** and TNFα (n=48) **(H)** in expanders who responded (exp-RE) and expanders who did not respond (exp-NR). Exact median values are reported. *P* values were calculated applying the Mann–Whitney test; ns=not significant, * $P<0.05$, ** $P<0.01$.

Supplementary Figure 25

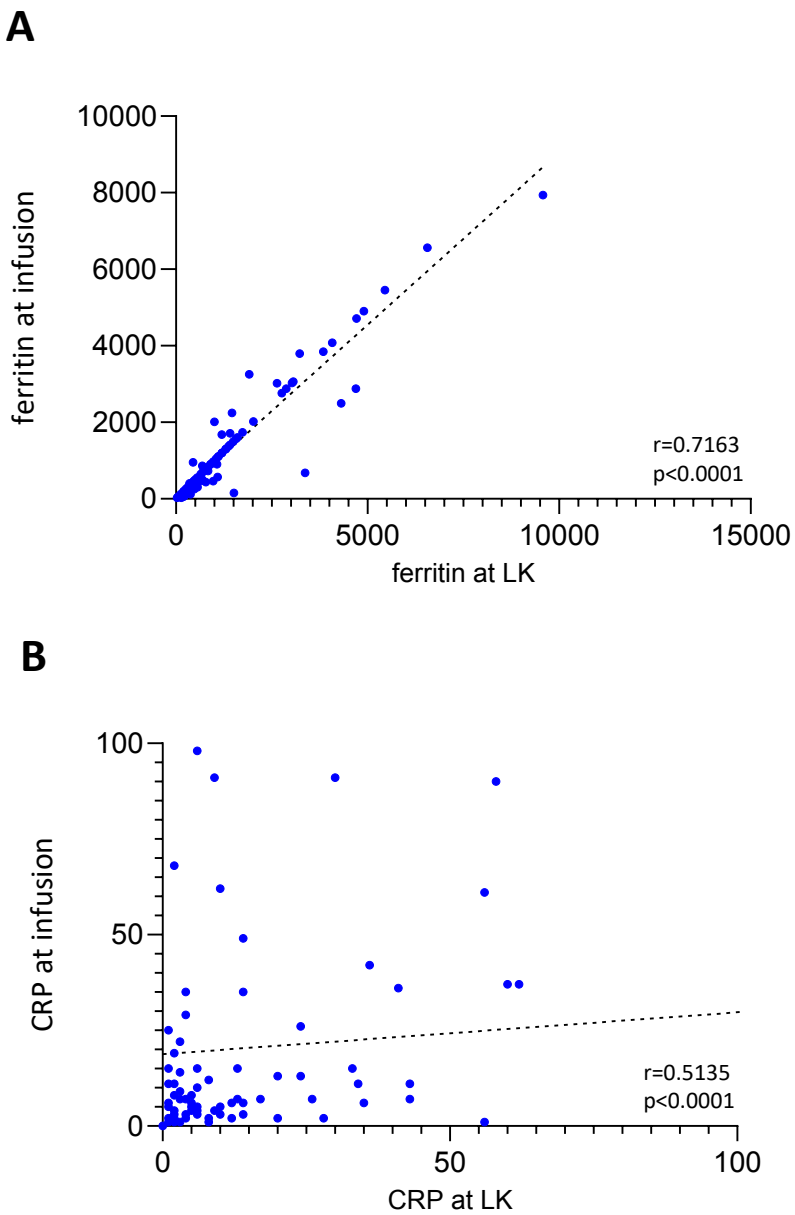

Supplementary Figure 25: Correlation betwee ferritin and C-reactive protein (CRP) levels at leukapheresis and at infusion.
A) Scatter dot plot showing the Spearman correlation between ferritin levels assessed at leukapheresis (LK) and at infusion (n=262). **B)** Scatter dot plot showing the Spearman correletion between CRP levels assessed at leukapheresis and at infusion (n=262).

Supplementary Figure 26

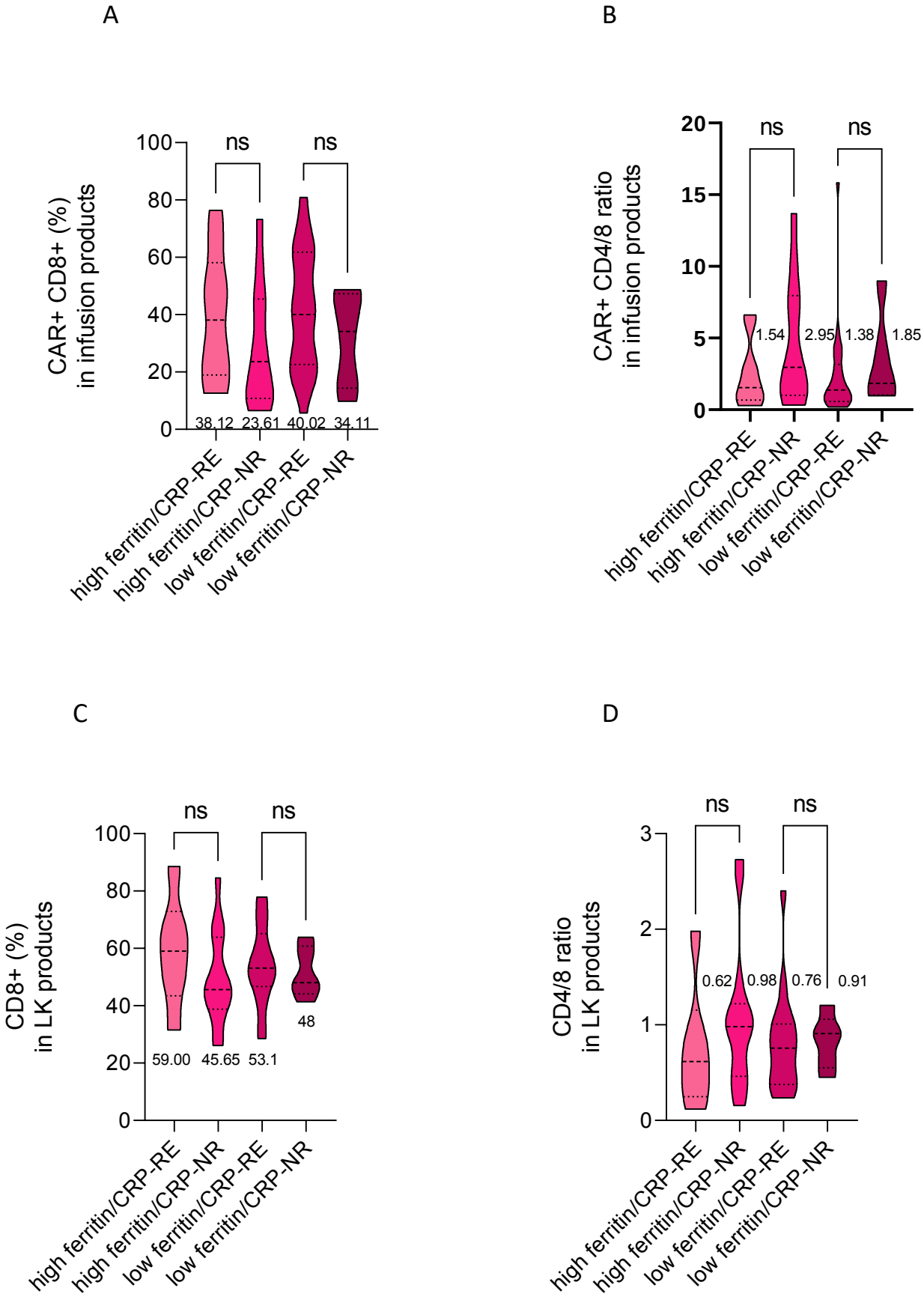

Supplementary Figure 26: Differences in CD8+ and CD4/CD8 ratio in infusion products and leukapheresis products, in relation to the levels of ferritin and C-reactive protein (CRP) and day 90 response.

Graphs showing the % of CAR+CD8+ cells **(A)** and the CAR+CD4/CD8 ratio **(B)** in infusion products (n=53). Graphs showing the % of CD8+ cells **(C)** and the CD4/CD8 ratio **(D)** in leukapheresis (LK) products (n=53). High ferritin/CRP: patients with ferritin and CRP levels higher than the median (406 ng/mL and 9 mg/L, respectively); low ferritin/CRP: patients with ferritin and CRP levels lower than the median. RE: responders by day 90, NR: non responders by day 90. Exact median values are reported. *P* values were calculated applying the Mann–Whitney test; ns=not significant.

Supplementary Figure 27

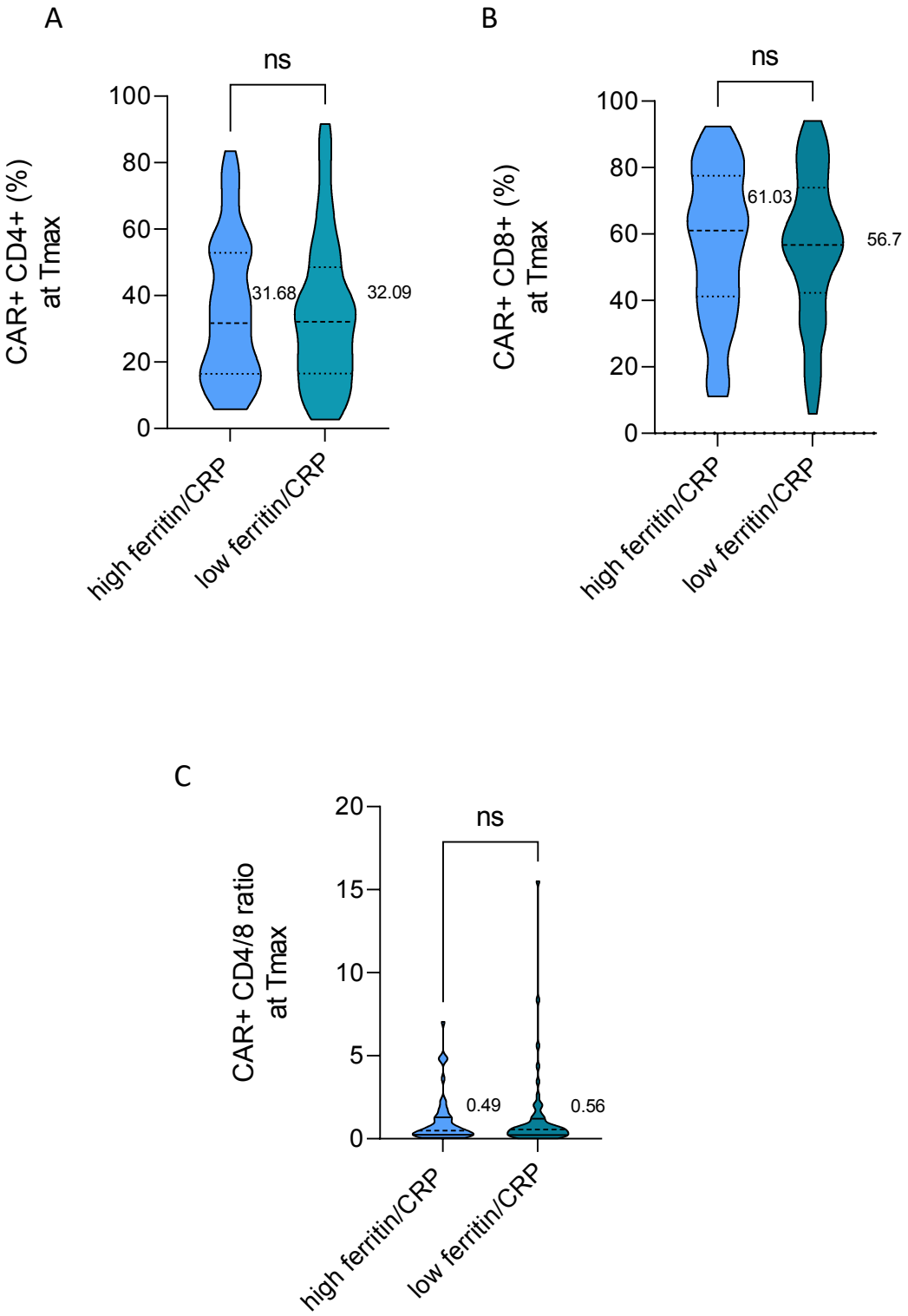

Supplementary Figure 27: Differences in CAR+CD8+, CAR+CD4+ and CAR+ CD4/CD8 ratio in relation to the levels of ferritin and C-reactive protein (CRP).
Graphs showing the % of CAR+CD8+ cells **(A),** the % of CAR+CD8+ cells **(B)**, and the CAR+CD4/CD8 ratio **(C)** at peak expansion (T_{max}). High ferritin/CRP: patients with both ferritin and CRP levels higher than the median (406 ng/mL and 9 mg/L, respectively); low ferritin/CRP: patients with both ferritin and CRP levels lower than the median (n=102). Exact median values are reported. *P* values were calculated applying the Mann–Whitney test; ns=not significant.

Supplementary table 1: Patients' characteristics, outcome and toxicities

Number of patients		262 pts
Age (median, range)		60 years (18-76)
Males		166 (63%)
Histotypes	DLBCL	152 (58%)
	tFL	40 (15%)
	HGBCL	42 (16%)
	PMBCL	28 (11%)
Prior lines	Prior lines >2 (3-6)	90 (34%)
	Prior ASCT	64 (24%)
Stage at LK	>II	179 (68%)
Bulky disease (>7.5cm) at LK		95 (36%)
Bridging therapy		221 (84%)
CRP >ULN at infusion		170 (65%)
Ferritin >ULN at infusion		147 (56%)
LDH >ULN at infusion		62 (30%) *
CAR T-cell product	axi-cel	168 (64%)
	tisa-cel	94 (36%)
CR at day 90		115 (44%) **
ORR at day 90		135 (56%) **
CRS	any grade	214 (82%)
	grade >1	70 (33%)
ICANS	any grade	94 (36%)

* *available for 204 patients*

** *available for 235 patients*

Abbreviations: ASCT: Autologous Stem Cell Transplant; CR: Complete Response; CRP: C-Reactive Protein; CRS: cytokine release syndrome; DLBCL: Diffuse Large B-cell Lymphoma; HGBCL: High Grade B-cell Lymphoma; ICANS: immune effector cell-associated neurotoxicity syndrome; LDH: Lactate Dehydrogenase; LK: leukapheresis; ORR: overall response rate; PMBCL: Primary Mediastinal B-cell Lymphoma; tFL: transformed Follicular Lymphoma; ULN: Upper Limit of Normal.

Supplementary table 2: Patients' characteristics, outcome and toxicities were representative of the broader LBCL cohort of the CART SIE study

Number of patients		**262 pts (this study)**	**640 pts (all LBCL CART SIE)**	P VALUE
Age (median, range)		60 (18-76)	59 (18-76)	ns
Males		166 (63%)	397 (62%)	ns
Histotypes	DLBCL	152 (58%)	363 (56%)	ns
	tFL	40 (15%)	106 (17%)	ns
	HGBCL	42 (16%)	91 (15%)	ns
	PMBCL	28 (11%)	79 (12%)	ns
Prior lines	Prior lines >2 (3-6)	90 (34%)	220 (34%)	ns
	Prior ASCT	64 (24%)	172 (27%)	
Stage at LK	>II	179 (68%)	439 (69%)	ns
Bulky disease (>7.5cm) at LK		95 (36%)	221 (35%)	ns
Bridging therapy		221 (84%)	526 (82%)	ns
CRP >ULN at infusion		170 (65%)	384 (60%)	ns
Ferritin >ULN at infusion		147 (56%)	274 (43%)	ns
LDH >ULN at infusion		62 (30%) *	159 (31%) **	ns
CAR T-cell product	axi-cel	168 (64%)	368 (57%)	ns
	tisa-cel	94 (36%)	272 (43%)	
CR at day 90		115 (44%) ***	262 (46%) ****	ns
ORR at day 90		135 (56%) ***	307 (61%) ****	ns
CRS	any grade	214 (82%)	538 (84%)	ns
	grade >1	70 (33%)	231 (43%)	ns
ICANS	any grade	94 (36%)	151 (24%)	ns

** available for 204 patients*
*** available for 508 patients*
**** available for 235 patients*
***** available for 564 patients*

Abbreviations: ASCT: Autologous Stem Cell Transplant; CR: Complete Response; CRP: C-Reactive Protein; CRS: cytokine release syndrome; LBCL: Large B-cell Lymphoma; DLBCL: Diffuse Large B-cell Lymphoma; HGBCL: High Grade B-cell Lymphoma; ICANS: immune effector cell-associated neurotoxicity syndrome; LDH: Lactate Dehydrogenase; LK: leukapheresis; ORR: overall response rate; PMBCL: Primary Mediastinal B-cell Lymphoma; tFL: transformed Follicular Lymphoma; ULN: Upper Limit of Normal.

Supplementary table 3: Sequence of primers and probes developed for CD19-CAR copies identification by ddPCR

anti-CD19 CAR T molecular assay	
forward	GTCTGGAGTGGCTGGGAGTA
probe	FAM- TCAGCTCTCAAATCCAGACTGACCA -BQH1
reverse	TTGGCTCTTGGAGTTGTCCT

Supplementary table 4: CAR T-cell biodistribution by ddPCR

Sample	CAR T product	CAR copies/µg DNA
BM	tisa-cel	440.9
BM	axi-cel	666.4
BM	axi-cel	366.2
BM	axi-cel	304.5
BM	tisa-cel	991.5
Tissue biopsy	tisa-cel	0.0
Tissue biopsy	tisa-cel	0.0
Tissue biopsy	axi-cel	375.4
Tissue biopsy	axi-cel	864.1
Tissue biopsy	tisa-cel	0.0
Ascitis	tisa-cel	6481.5
cfDNA	axi-cel	9672.2
cfDNA	axi-cel	27934.0
cfDNA	axi-cel	2350.2
cfDNA	axi-cel	2201
cfDNA	axi-cel	3438.9
cfDNA	axi-cel	2728.9
cfDNA	axi-cel	4643.3
cfDNA	axi-cel	0.0

Abbreviations: BM: bone marrow; cfDNA: cell free DNA.

Supplementary table 5: Univariable logistic models for CRS

Univariable logistic models for CRS					
Variable	**OR**	**Lower 0.95**	**Upper 0.95**	**Overall p-value**	**Non-linear p-value**
C_{10}	1.28	0.89	1.83	0.1807	
Non-linear C_{10}	5.01	1.89	13.26	0.0045	0.0021
C_{10} with respect to median	3.38	1.51	7.56	0.0031	
C_{10} with respect to ROC curve cut-off*	4.80	2.13	10.83	0.0002	
C_{max}	1.89	1.13	3.16	0.0149	
Non-linear C_{max}	4.47	2.00	9.98	0.0004	0.0030
C_{max} with respect to median	3.31	1.66	6.61	0.0007	
C_{max} with respect to ROC curve cut-off**	3.63	1.87	7.04	0.0001	
AUC_{0-30}	2.35	1.29	4.28	0.0054	
Non-linear AUC_{0-30}	4.82	2.13	10.91	0.0002	0.0072
AUC_{0-30} with respect to median	3.76	1.85	7.62	0.0002	
AUC_{0-30} with respect to ROC curve cut-off***	4.73	2.33	9.62	<0.0001	

* Cut-off value: 16.71 (AUC=71.36%, sensitivity=64.89, specificity=72.22)
** Cut-off value: 26.42 (AUC=71.68%, sensitivity=64.49, specificity=66.67)
*** Cut-off value: 69.805 (AUC=72.91%, sensitivity=61.21, specificity=75)

Abbreviations: AUC_{0-30}: median cumulative CAR T level within the first month; C_{10}: median CAR T count at day 10 post-infusion; C_{max}: median CAR T count at peak expansion; CRS: cytokine release syndrome; OR: odds ratio; ROC: receiver operating characteristic.

Supplementary table 6: Univariable logistic models for ICANS

Univariable logistic models for ICANS					
Variable	**OR**	**Lower 0.95**	**Upper 0.95**	**Overall p-value**	**Non-linear p-value**
C_{10}	1.17	0.99	1.38	0.0698	
Non-linear C_{10}	1.84	0.91	3.72	0.0656	0.1852
C_{10} with respect to median	2.63	1.33	5.20	0.0053	
C_{10} with respect to ROC curve cut-off*	2.81	1.40	5.63	0.0035	
C_{max}	1.18	1.04	1.34	0.0125	
Non-linear C_{max}	1.05	0.62	1.80	0.0492	0.6782
C_{max} with respect to median	1.34	0.81	2.22	0.2607	
$C_{max}$with respect to ROC curve cut-off**	1.68	1.00	2.83	0.0517	
AUC_{0-30}	1.21	1.05	1.40	0.0104	
Non-linear AUC_{0-30}	1.08	0.62	1.87	0.0383	0.6737
AUC_{0-30} with respect to median	1.53	0.92	2.55	0.1013	
AUC_{0-30} with respect to ROC curve cut off***	1.63	0.98	2.72	0.0611	

* Cut-off value: 18.48 (AUC=60.92%, sensitivity=69.81, specificity=54.87)
** Cut-off value: 27 (AUC=56.58%, sensitivity=65.96, specificity=47.59)
*** Cut-off value: 76.555 (AUC=56.49%, sensitivity=58.51, specificity=53.61)

Abbreviations: AUC_{0-30}: median cumulative CAR T level within the first month; C_{10}: median CAR T count at day 10 post-infusion; C_{max}: median CAR T count at peak expansion; ICANS: immune effector cell-associated neurotoxicity syndrome; OR: odds ratio; ROC: receiver operating characteristic.

Supplementary table 7: Univariable logistic models for ORR at day 90

Univariable logistic models for ORR at day 90					
Variable	**OR**	**Lower 0.95**	**Upper 0.95**	**Overall p-value**	**Non-linear p-value**
C_{10}	1.13	0.94	1.35	0.1877	
Non-linear C_{10}	1.81	0.92	3.56	0.1324	0.1505
C_{10} with respect to median	1.77	0.94	3.34	0.0786	
C_{10} with respect to ROC curve cut-off *	2.14	1.12	4.07	0.0210	
C_{max}	1.06	0.94	1.20	0.3104	
Non-linear C_{max}	2.08	1.20	3.59	0.0282	0.0134
C_{max} with respect to median	1.92	1.14	3.23	0.0146	
C_{max} with respect to ROC curve cut-off **	2.55	1.50	4.36	0.0006	
AUC_{0-30}	1.11	0.95	1.30	0.1790	
Non-linear AUC_{0-30}	2.25	1.27	3.98	0.0167	0.0115
AUC_{0-30} with respect to median	1.92	1.14	3.23	0.0146	
AUC_{0-30} with respect to ROC curve cut-off ***	1.98	1.17	3.33	0.0106	

* Cut-off value: 16.71 (AUC=59.62%, sensitivity=65.06, specificity=53.42)
** Cut-off value: 25.78 (AUC=61.06%, sensitivity=69.47, specificity=52.88)
*** Cut-off value: 77.77(AUC=61.34%, sensitivity=57.25, specificity=59.62)

Abbreviations: AUC_{0-30}: median cumulative CAR T level within the first month; C_{10}: median CAR T count at day 10 post-infusion; C_{max}: median CAR T count at peak expansion; OR: odds ratio; ORR: overall response rate; ROC: receiver operating characteristic.

Supplementary table 8: Univariable Cox models for PFS

Univariable Cox models for PFS					
Variable	**HR**	**Lower 0.95**	**Upper 0.95**	**Overall p-value**	**Non-linear p-value**
C_{10}	0.89	0.78	1.02	0.0881	
Non-linear C_{10}	0.70	0.45	1.09	0.0918	0.2509
C_{10} with respect to median	0.69	0.46	1.04	0.0741	
C_{10} with respect to ROC curve cut-off*	0.84	0.55	1.29	0.4306	
C_{max}	0.94	0.87	1.03	0.1820	
Non-linear C_{max}	0.62	0.44	0.88	0.0205	0.0154
C_{max} with respect to median	0.60	0.43	0.84	0.0025	
C_{max} with respect to ROC curve cut-off**	0.71	0.50	1.00	0.0518	
AUC_{0-30}	0.91	0.82	1.01	0.0862	
Non-linear AUC_{0-30}	0.62	0.44	0.89	0.0174	0.0294
AUC_{0-30} with respect to median	0.66	0.48	0.91	0.0126	
AUC_{0-30} with respect to ROC curve cut-off***	0.70	0.51	0.97	0.0338	

* Cut-off value: 11.55 (AUC=40%, sensitivity=64.7, specificity=28.45)
** Cut-off value: 62.64 (AUC=38.35%, sensitivity=31.51, specificity=54.01)
*** Cut-off value: 72.05 (AUC=39.43%, sensitivity=47.18, specificity=39.24)

Abbreviations: AUC_{0-30}: median cumulative CAR T level within the first month; C_{10}: median CAR T count at day 10 post-infusion; C_{max}: median CAR T count at peak expansion; HR: hazard ratio; ROC: receiver operating characteristic; PFS: progression-free survival.

Supplementary table 9: Univariable Cox models for OS

Univariable Cox models for OS					
Variable	**HR**	**Lower 0.95**	**Upper 0.95**	**Overall p-value**	**Non-linear p-value**
C_{10}	0.85	0.68	1.06	0.1455	
Non-linear C_{10}	0.91	0.49	1.68	0.3795	0.7957
C_{10} with respect to median	0.83	0.49	1.42	0.4956	
C_{10} with respect to ROC curve cut-off*	0.70	0.40	1.25	0.2297	
C_{max}	0.97	0.87	1.08	0.5856	
Non-linear C_{max}	0.67	0.43	1.06	0.2311	0.1013
C_{max} with respect to median	0.68	0.45	1.04	0.0749	
C_{max} with respect to ROC curve cut-off**	0.76	0.49	1.20	0.2365	
AUC_{0-30}	0.93	0.81	1.07	0.3196	
Non-linear AUC_{0-30}	0.65	0.41	1.04	0.1660	0.1120
AUC_{0-30} with respect to median	0.69	0.46	1.06	0.0921	
AUC_{0-30} with respect to ROC curve cut-off***	0.68	0.45	1.05	0.0796	

* Cut-off value: 30.8 (AUC=49.34%, sensitivity=41.19, specificity=61.84)
** Cut-off value: 32.9 (AUC=45.49%, sensitivity=48.48, specificity=45.65)
*** Cut-off value: 80.59 (AUC=45.03%, sensitivity=45.35, specificity=49.18)

Abbreviations: AUC_{0-30}: median cumulative CAR T level within the first month; C_{10}: median CAR T count at day 10 post-infusion; C_{max}: median CAR T count at peak expansion; HR: hazard ratio; ROC: receiver operating characteristic; OS: overall survival.

Supplementary table 10: Univariable logistic models for ORR at day 90

Univariable logistic models for ORR at day 90				
Variable	**OR**	**Lower 0.95**	**Upper 0.95**	**p-value**
Age	1.49	0.89	2.5	0.1195
Sex - Female vs. Male	1.65	0.95	2.87	0.077
Histology - HGBCL vs. DLBCL	0.75	0.39	1.44	0.0182
Histology - PMBCL vs. DLBCL	3.74	1.35	10.37	NA
Transformed vs. non-transformed LBCL	3.46	1.54	7.76	0.0003
Number of previous lines	0.93	0.68	1.27	0.6497
Disease status - Refractory vs. Relapsed	0.9	0.47	1.72	0.7557
ASCT - Yes vs. No	1.75	0.95	3.25	0.074
Ann Arbor - III-IV vs. I-II	0.47	0.26	0.86	0.0147
Bulky - Yes vs. No	0.93	0.54	1.6	0.7917
Extranodal - Yes vs. No	0.5	0.29	0.87	0.0139
IPI - High vs. Low	0.96	0.56	1.63	0.8769
CAR T product - Tisa vs. Axi	0.53	0.31	0.91	0.0203
Bridging therapy - Yes vs. No	1.07	0.52	2.2	0.8506
Response to bridge - RE vs. NR	2.48	1.4	4.4	0.0019
Pre infusion monocytes	0.95	0.54	1.66	0.3352
Pre infusion LDH	0.53	0.34	0.82	0.0047
Pre infusion CRP	0.45	0.26	0.81	0.0126
Pre infusion ferritin	0.32	0.17	0.59	0.0000
Pre infusion IL6	0.56	0.18	1.72	0.1203
Pre infusion IL18	0.74	0.26	2.05	0.1871
Pre infusion IL11	0.84	0.32	2.2	0.9297
Pre infusion IL1beta	0.14	0	30.22	0.6564
Pre infusion TNFalpha	1.39	0.53	3.68	0.4601
Pre infusion IFNgamma	0.99	0.44	2.2	0.7438
Pre infusion TGFbeta	1.5	0.38	5.91	0.3374
Pre infusion IL10	0.64	0.32	1.28	0.2333
Expander - strong:poor	1.92	1.14	3.23	0.0146

Abbreviations: ASCT: Autologous Stem Cell Transplant; CRP: C-Reactive Protein; DLBCL: Diffuse Large B-cell Lymphoma; HGBCL: High Grade B-cell Lymphoma; LBCL: Large B-cell Lymphoma; IPI: international prognostic index; LDH: Lactate Dehydrogenase; LBCL: Large B-cell Lymphoma; PMBCL: Primary Mediastinal B-cell Lymphoma; RE: responders; NR: non-responders; OR: odds ratio; ORR: overall response rate.

Supplementary table 11: Univariable Cox models for PFS

Univariable Cox models for PFS				
Variable	**HR**	**Lower 0.95**	**Upper 0.95**	**p-value**
Age	0.97	0.71	1.32	0.0967
Sex - Female vs. Male	0.78	0.55	1.11	0.1697
Histology - HGBCL vs. DLBCL	1.1	0.74	1.63	0.0165
Histology - PMBCL vs. DLBCL	0.36	0.18	0.75	NA
Transformed vs. non-transformed LBCL	0.63	0.39	1.01	0.0025
Number of previous lines	1.01	0.83	1.24	0.8917
Disease status - Refractory vs. Relapse	1.02	0.69	1.51	0.9252
ASCT - Yes vs. No	0.66	0.44	0.99	0.0452
Ann Arbor - III-IV vs. I-II	1.55	1.05	2.28	0.0257
Bulky - Yes vs. No	1.05	0.75	1.47	0.7743
Extranodal - Yes vs. No	1.39	0.98	1.95	0.0619
IPI - High vs. Low	1.16	0.83	1.62	0.3781
CAR T product - Tisa vs. Axi	1.62	1.17	2.25	0.0036
Bridging therapy - Yes vs. No	0.85	0.54	1.33	0.4742
Response to bridge - RE vs. NR	0.58	0.4	0.84	0.0036
Pre infusion LDH	1.61	1.19	2.16	0.0000
Pre infusion CRP	1.66	1.19	2.34	0.0019
Pre infusion ferritin	1.39	0.96	2	0.0005
Pre infusion monocytes	1.22	0.85	1.75	0.017
Pre infusion IL6	1.53	0.8	2.94	0.0525
Pre infusion IL18	1.78	0.92	3.44	0.0966
Pre infusion IL11	0.68	0.36	1.29	0.488
Pre infusion IL1beta	2.34	0.23	23.37	0.7454
Pre infusion TNFalpha	1.16	0.61	2.2	0.2074
Pre infusion IFNgamma	1.04	0.61	1.77	0.9462
Pre infusion TGFbeta	0.72	0.32	1.63	0.0558
Pre infusion IL10	1.26	0.83	1.92	0.0584
Expander - strong:poor	0.66	0.48	0.91	0.0126

Abbreviations: ASCT: Autologous Stem Cell Transplant; CRP: C-Reactive Protein; DLBCL: Diffuse Large B-cell Lymphoma; HGBCL: High Grade B-cell Lymphoma; PMBCL: Primary Mediastinal B-cell Lymphoma; HR: hazard ratio; IPI: international prognostic index; LDH: Lactate Dehydrogenase; LBCL: Large B-cell Lymphoma; RE: responders; NR: non-responders; PFS: progression-free survival.

Supplementary table 12: Bivariable models to assess the interaction between CAR T product and expansion on overall response at day 90

Expansion effect in Axi-cel

Variable	OR	Lower 0.95	Upper 0.95
cart_product - Tisa:Axi	0.45	0.21	0.96
auc_cat - strong:poor	1.67	0.85	3.27

Expansion effect in Tisa-cel

Variable	OR	Lower 0.95	Upper 0.95
auc_cat - strong:poor	2.35	1	5.52

Variable	p.value
CAR-T product	0.0649
Expander	0.0479
Interaction CAR-T product x expander	0.5339

Abbreviations: OR: Odds Ratio

Supplementary table 13: Bivariable models to assess the interaction between CAR T product and expansion on progression-free survival (PFS)

Expansion effect in Axi-cel

Variable	HR	Lower 0.95	Upper 0.95
cart_product - Tisa:Axi	1.68	1.09	2.58
auc_cat - strong:poor	0.68	0.44	1.06

Expansion effect in Tisa-cel

Variable	HR	Lower 0.95	Upper 0.95
auc_cat - strong:poor	0.63	0.39	1.04

Variable	p.value
CAR-T product	0.0144
Expander	0.0446
Interaction CAR-T product x expander	0.8166

Abbreviations: HR: Hazard Ratio

Supplementary table 14: Bivariable models to assess the role of ferritin, CRP and LDH on overall response at day 90

Ferritin effect in poor expanders

Variable	OR	Lower 0.95	Upper 0.95
ferritin	0.75	0.52	1.09
auc_cat - strong:poor	2.63	1.41	4.91

Ferritin effect in strong expanders

Variable	OR	Lower 0.95	Upper 0.95
ferritin	0.4	0.24	0.67

Variable	p.value
Ferritin	0.0009
Expander	0.0057
Interaction ferritin x expander	0.0546

CRP effect in poor expanders

Variable	OR	Lower 0.95	Upper 0.95
crp	1.00	0.78	1.28
auc_cat - strong:poor	2.85	1.58	5.13

CRP effect in strong expanders

Variable	OR	Lower 0.95	Upper 0.95
crp	0.7	0.53	0.94

Variable	p.value
CRP	0.0538
Expander	0.0019
Interaction CRP x expander	0.0685

LDH effect in poor expanders

Variable	OR	Lower 0.95	Upper 0.95
ldh_normalized	0.65	0.41	1.05
auc_cat - strong:poor	2.01	1.07	3.74

LDH effect in strong expanders

Variable	OR	Lower 0.95	Upper 0.95
ldh_normalized	0.85	0.69	1.04

Variable	p.value
LDH	0.0599
Expander	0.0273
Interaction LDH x expander	0.3281

Abbreviations: CRP: C-reactive Protein; LDH: lactate dehydrogenase; OR: Odds Ratio

Supplementary table 15: Bivariable models to assess the role of ferritin, CRP and LDH on overall survival

Ferritin effect in poor expanders

Variable	HR	Lower 0.95	Upper 0.95
ferritin	1.25	1.08	1.46
auc_cat - strong:poor	0.59	0.35	0.98

Ferritin effect in strong expanders

Variable	HR	Lower 0.95	Upper 0.95
ferritin	1.54	1.34	1.76

Variable	p.value
Ferritin	0.0000
Expander	0.0627
Interaction ferritin x expander	0.0454

CRP effect in poor expanders

Variable	HR	Lower 0.95	Upper 0.95
crp	1.14	1.02	1.27
auc_cat - strong:poor	0.57	0.35	0.91

CRP effect in strong expanders

Variable	HR	Lower 0.95	Upper 0.95
crp	1.28	1.15	1.43

Variable	p.value
CRP	0.0000
Expander	0.0557
Interaction CRP x expander	0.1294

LDH effect in poor expanders

Variable	HR	Lower 0.95	Upper 0.95
ldh_normalized	1.33	1.2	1.48
auc_cat - strong:poor	0.69	0.4	1.17

LDH effect in strong expanders

Variable	HR	Lower 0.95	Upper 0.95
ldh_normalized	1.23	1.12	1.35

Variable	p.value
LDH	0.0000
Expander	0.0683

Variable	p.value
Interaction LDH x expander	0.2232

Abbreviations: CRP: C-reactive Protein; LDH: lactate dehydrogenase; HR: Hazard Ratio

Supplementary table 16: Bivariable models to assess the role of ferritin, CRP LDH on progression-free survival

Ferritin effect in poor expanders

Variable	HR	Lower 0.95	Upper 0.95
ferritin	1.10	0.97	1.25
auc_cat - strong:poor	0.55	0.37	0.80

Ferritin effect in strong expanders

Variable	HR	Lower 0.95	Upper 0.95
ferritin	1.34	1.18	1.52

Variable	p.value
Ferritin	0.0000
Expander	0.0049
Interaction ferritin x expander	0.0342

CRP effect in poor expanders

Variable	HR	Lower 0.95	Upper 0.95
crp	1.05	0.94	1.18
auc_cat - strong:poor	0.57	0.40	0.82

CRP effect in strong expanders

Variable	HR	Lower 0.95	Upper 0.95
crp	1.17	1.06	1.29

Variable	p.value
CRP	0.0043
Expander	0.0100
Interaction CRP x expander	0.1764

LDH effect in poor expanders

Variable	HR	Lower 0.95	Upper 0.95
ldh_normalized	1.24	1.14	1.36
auc_cat - strong:poor	0.62	0.42	0.91

LDH effect in strong expanders

Variable	HR	Lower 0.95	Upper 0.95
ldh_normalized	1.12	1.02	1.22

Variable	p.value
LDH	0.0000
Expander	0.0027

Variable	p.value
Interaction LDH x expander	0.0933

Abbreviations: CRP: C-reactive Protein; LDH: lactate dehydrogenase; HR: Hazard Ratio

Supplementary table 17: Spearman's correlations among IL-6, IL-10, IL-18 and pre-infusion C-reactive protein (CRP) and ferritin levels

correlation	Spearman r	P value
CRP / IL-6	0.5276	0.0001
CRP / IL-10	0.3775	0.0015
CRP / IL-18	0.3426	0.0035
ferritin / IL-6	0.2534	0.0317
ferritin / IL-10	0.2667	0.0279
ferritin / IL-18	0.3309	0.0048

References

1. Monfrini C, Stella F, Aragona V, et al. Phenotypic Composition of Commercial Anti-CD19 CAR T Cells Affects In Vivo Expansion and Disease Response in Patients with Large B-cell Lymphoma. Clin Cancer Res 2022;OF1–OF9.
2. Carniti C, Caldarelli NM, Agnelli L, et al. Monocytes in leukapheresis products affect the outcome of CD19-targeted CAR T-cell therapy in lymphoma patients. Blood Adv [Epub ahead of print]